MODIFICATION OF N95 RESPIRATORS: ALLAYING DEFICITS IN RESPIRATORY PROTECTION BELOW 300 NANOMETERS

by

ADAM NORED

DANEESH SIMIEN, COMMITTEE CHAIR
PHIL DEMOKRITOU
ROBIN FOLEY
ILIAS KAVOURAS
CLAUDIU LUNGU

A DISSERTATION

Submitted to the graduate faculty of the University of Alabama at Birmingham,
in partial fulfillment of the requirements for the degree of
Doctor of Philosophy

BIRMINGHAM, ALABAMA

2021

MODIFICATION OF N95 RESPIRATORS: ALLAYING DEFICITS IN RESPIRATORY PROTECTION BELOW 300 NANOMETERS

ADAM NORED

INTERDISCIPLINARY ENGINEERING

ABSTRACT

The current growth rate of nanomaterials being used in everyday materials as well as in construction materials is quite large. While this in itself could be quite promising, there is a lack of information known about the risks that materials in the nano size range may have attached to their use. Until a full-scale risk analysis of the nanomaterials is used in the construction industry there is a need for personal protection to be implemented. A known issue with the current PPE exists, in that the N95 personal respirator has some particle collection efficiency issues below 300 nm. Modifications to increase the particle collection efficiency of the N95 below 300 nm is the subject of this research.

Before modifications were to occur, chemical and morphological properties of paints containing TiO_2 during end-of-life procedures were determined, to fully understand the likelihood of worker exposure to particles under 300 nm. General testing as well as a one-year weathering study were undertaken to create an understanding of short- and long-term effects on the possibility of nano-sized particles being generated during the end-of-life procedures as well as the possibility of the generated particles being TiO_2 in whole or in part. This was determined by collecting data on the size of particles generated, and the number of particles generated within size ranges. Upon

determination that there was a real concern, the plan for modification of the N95 moved forward.

Three different filters were examined and tested during the study, to determine the best pairing of current filters and additions. The filter types that were focused on are the ones commonly found in laboratory air sampling due to these being created to collect low end PM. The addition of cellulose acetate or PTFE filters was determined to help solve the current N95 respirator's issues with particles under 300 nm.

Keywords: N95 respirator, PPE, filter, collection efficiency

DEDICATION

To my father, R.W. Miss you dad.

ACKNOWLEDGEMENTS

I would like to acknowledge Dr. Kavouras. You helped guide and push me to a place where I could finish this doctorate, even when I had reached a point I did not know if I wanted to continue. Thanks for everything, especially when you changed schools and kept working with me, which you said was your duty, but I have heard of several mentors who did not, and it means the world to me.

I would also like to thank Dr. Simien for being my chair, the rest of my committee, Dr. Demokritou, Dr. Lungu, and Dr. Foley. Thank you for providing me your knowledge and expertise. Thank you for agreeing to be on my committee.

And finally, I would like to thank my family and especially my cohort members, Jake Shedd, Boyi Guo, Jordan Nelson, Olawabunmi Dada, and Margaret Summers. Thank you for your comfort and support. Your kind words and motivation have made it possible for me to drive this flying umbrella.

TABLE OF CONTENTS

LIST OF TABLES

LIST OF FIGURES

THE EFFECT OF PARTICLE SIZE, MEMBRANE TYPE, AND FACE VELOCITY ON TIO_2-CONTAINING PAINT DUST FILTRATION

LIST OF ABBREVIATIONS

AQS	Air Quality System
ATR-FTIR	Attenuated Total Reflectance Fourier-Transform Infrared Spectrometer
CARES	Coatings Aerosol Resuspension System
CDC	Center for Disease Control
CI	Confidence Interval
CMD	Count Median Diameter
COPD	Chronic Obstructive Pulmonary Disease
CPC	Condensation Particle Counter
CV	Coefficient of Variance
d_a	Aerodynamic Diameter
DMA	Differential Mobility Analyzer
EDS	Energy Dispersive Spectroscopy
ENM	Engineered Nanomaterials
EPA	Environmental Protection Agency
FFR	Filtering Facepiece Respirator
FP	Fine Particles
GSD	Geometric Standard Deviation
HEPA	High-Efficiency Particulate Filter

IARC	International Agency for Research on Cancer
ICPMS	Inductively Coupled Plasma Mass Spectrometry
LPM	Liters Per Minute
MMD	Mass Median Diameter
MPPS	Most Penetrating Particle Size
NEP	Nano-Enabled Products
NIOSH	National Institute of Occupational Health and Safety
nm	Nanometer
NP	Nanoparticle
OEL	Occupational Exposure Limit
OSHA	Occupational Safety and Health Agency
P_{120}	120 Grit sandpaper
P_{220}	220 Grit sandpaper
P_{40}	40 Grit sandpaper
PEL	Permissible Exposure Limit
PM	Particulate Matter
Pm	Penetration
PM0.1	Nano-size Particulates
PM1.0	Accumulation-mode Particulates
PM10	Thoracic Particulates
PM2.5	Fine Particulates
PNC	Particle Number Concentrations
PPE	Personal Protective Equipment

PTFE	Polytetrafluoroethylene
QCM	Quartz Crystal Microbalance
REL	Recommended Exposure Limit
SEM	Scanning Electron Microscope
TiO_2	Titanium Dioxide
TSP	Total Suspended Particles
TWA	Time Weighted Average
UV	Ultra-Violet
WPS	Wide-range Particle Scanner

INTRODUCTION

Engineered nanomaterials (hereafter known as ENMs) are chemicals, composites, metals, and metal oxides that are manufactured into various shapes that are less than 100 nanometers an all three axes. [1] The physical properties of ENMs that are typically present in microparticles, differ to those of the bulk chemical because of the increase in the ratio of surface-area-to-volume and quantum effects. As particle size decreases, the behavior of atoms on the surface of the particles is the driving mechanism for the interactions with other materials, leading to enhanced characteristics such as strength, chemical and/or heat resistance. Nano-sized particles may also exhibit quantum mechanical behavior including quantum dots with characteristics comparable to semiconductors. Finally, ENMs are transparent because their size is lower than the wavelengths within the visible spectrum (300-500 nm).

ENMs have been integrated in numerous nano-enabled products (NEPs) including paint coatings with a variety of submicron/nanoscale pigments (metals and metal-oxides), toner formulations, nanocomposites, carbon nanotubes, sintered compacts made of metal and oxide nanoparticle, super-hard coatings with films of refractory nitrides, carbides, and diamond like coating nanolayers. NEPs are currently used across many industries including agriculture, aerogels, aerospace, automotive, catalysts, coatings, paints, and pigments.

The construction industry has over seven million employees that creates over a trillion dollars of infrastructure and other buildings a year. Innovation is a key driver to stay at the forefront of the profession. One of the newest innovations in construction technology is incorporation of ENMs within construction materials. First introduced into consumer products in the early 2000s, ENMs have expanded to be included in many construction materials, including concrete, insulation, solar cells, steel, and coating materials such as paint. [2]

Paints and coatings contain many solvents, pigments, extenders, and binders. Because of the use of water-based paints and powder coatings, several hazardous chemicals including benzene, phthalates, chromium, and lead oxides have been reduced or replaced in paint. [3] New formulations contain lower-toxicity solvents and neutralizing agents, such as amines, and biocides. ENMs have been incorporated as free powders, stabilized particles in suspensions or mixed into paint batches or granulates. [4] As a result, coatings and paints have gained many useful traits; these include increased durability, strength, fire resistance, biocidal activity, and the ability to self-clean. [4–7] The ENMs typically used in paints are: TiO_2, silicon dioxide (SiO_2), ZnO, copper oxide (CuO), Ag, cerium (IV) oxide (CeO_2), aluminum oxide (Al_2O_3), and iron oxide (Fe_2O_3). [4,6,7] TiO_2 is used for its biocidal properties. [8] It is also used in most base paint as the white pigment. SiO_2 is used for its scratch protection capabilities and dirt repellant [7], ZnO is used as a water and UV protectant. [7,9] CuO is an antifouling agent and is mainly used on boat hulls. [10] Ag is an antimicrobial [11], CeO_2 protects from UV light [12], and Fe_2O_3 adds abrasion resistance. [4] In paints, nanoparticles form agglomerates with polymers [9], however, the integrity of these agglomerates may be compromised by

environmental and mechanical factors resulting in dislocation and release of nanoparticles over time. [13] TiO_2 is the most used (70% of the total pigments) white pigment in paints for their high stability, anticorrosive and biocidal properties. It is also the most commonly produced ENM at 10,000 tons a year. [14] TiO_2 exists in different particle size fractions as fine particles (FPs) (diameter 0.1-2.5 μm) and nanoparticles (NPs; diameter <0.1 μm).

ENVIRONMENTAL IMPACTS

A building has an average lifetime expectancy of 80 years. [15] In that time, it will be exposed to a gamut of weather conditions. The long-term exposure may have also been a pathway for the nanoparticles to enter the surrounding environment. Weathering experiments showed the run-off release of Ag ENMs, but not the release of TiO_2 nanoparticles, possibly relating to molecular interaction within the NEPs. [11,16] Kaegi et al. [11] estimated that up to 30% of Ag ENMs in paints may be released from outdoor facades in a year. Other ENMs may have just as high a release.

In addition to the release of nanoparticles in paint due to environmental weathering; repairs, renovations, demolition, and disposal of old materials covered in nano-enabled paints can lead to the release of nanoparticles in the environment in paint dust and/or solid wastes. [3] Direct exposures by inhalation of pristine (free of any other material) nanoparticles during paint manufacturing and application is speculated to be limited due to agglomerate formation and stabilization with paint polymers. The integrity of the paint agglomerates may be compromised over time and/or at the end of the product lifecycle leading to the release of nanoparticles from painted surfaces in the environment

by abrasion and weathering. This would lead to either environmental exposure due to weathering or worker exposure via abrasion.

Another aspect of the natural weathering study is the presence of acid deposition. The location for our study has been known to have elements in the air known to be components of acid deposition, such as nitrous oxides and sulfur dioxide. Their presence needed to be acknowledged and accounted for in our study. The interactions between TiO_2 and a wide range of acids has been studied thoroughly, with the acids largely and effectively destroyed by UV reaction with TiO_2 [17–19] The photocatalysis reaction that causes the destruction also seems to have a harmful effect on the nano-enabled coatings. The UV radiation of anatase Ti, the type mostly used for ENMs, causes a breakdown in the coatings themselves, allowing more TiO_2 to come to the surface, potentially allowing other weathering effects to remove more ENMs from the coatings over time, at a faster rate than previously thought. [20]

An issue with the widespread use of nanoparticles in construction materials in general, and paint in specific, is the lack of research into possible side effects of exposure to incidental nanoparticles. Incidental nanoparticles occur during daily activities that happen everywhere. [14] These nanoparticles also have been shown to influence the environment when introduced. They may enter environmental media (i.e., air, water, and soil) through intentional application or use of products containing nanoparticles (e.g., pesticides and fertilizers), or unintentional and accidental releases. Unintentional releases include runoff, wastewater treatment byproducts and disposal, solid waste mismanagement, and exterior paint degradation. TiO_2 ENMs have been tried in concrete mixes recently, to help remove pollutants on roadways. [21] With TiO_2 being added to a

product that is routinely broken down do to use, the odds of the ENMs being introduced into the local environment increases. Gottschalk et al. [22] reported the detection of Ag, TiO_2, and ZnO in treated wastewater, sediment, and effluent. Some plants and vegetation may have been shown to uptake nanoparticles. [23,24] Translocation of nanoparticles into edible and reproductive parts of crops is of concern because they can move further in the food chain affecting animals and humans. There have also been examples of animals up taking ENMs in waterways. [24] Nanoparticles suspended in water can also be toxic to aquatic organisms, fisheries, and animals. [24] TiO_2 has been shown to be a carcinogen, and also leads to cell death as an ENM. [25] TiO_2 as an aerosol has even been shown to create tumors in mouse lungs in doses below occupational exposure levels. Studies into ENM exposure to ecosystems are relatively unexplored or contradictory in their findings. However, it has been determined that TiO_2 ENMs cannot enter the body through the skin, so inhalation, and other uptake through consumed food and water are areas that need further study. [25]

HUMAN HEALTH IMPACTS

There are three main points at which a painter may be exposed to the nanoparticles in paint, the preparation, the application, and the removal of old paint. The application is usually unlikely to expose the workers to nanoparticles. Kaiser et al. [26] showed that ingestion of nanoparticle doped paint had the same effects as the ingestion of non-doped paint. During both application and removal, the main route of exposure to nanoparticles is through the airway. Nanoparticles, due to their size, are very likely to end up in the alveolar region of the lungs. [27] There is no body function to help remove

particles when they reach that low in the lung, so particles may sit there for months to years, and may possibly translocate. Because of their size, nanoparticles can move freely through cells and cause harm through oxidative stress and damage to the cell structure. [5] They can also cross into the blood stream and translocate into different parts of the body including the brain. [28] Effects to other organs, including liver, spleen, and kidney have also been reported. [5] They are shown to induce fibrosis, emphysema and tumors in the respiratory tract, neurodegenerative diseases, diminish the defense ability of the immune system, damage lymphocytes, participate in thrombosis, and cardiovascular diseases. [5,29,30] They also have been shown to increase the rate of pneumoconiosis. [31] It is noteworthy that the toxicity of nanoparticles may be influenced by size and shape. [5] Nanoparticles that are known to be in paint products have a wide range of possible side effects.

The risk for nanoparticle exposure seems to be higher for certain professions that encounter aerosols that possibly contain particulates. Painters are particularly more likely than many professions to be exposed to air born particulates. According to the US Bureau of Labor Statistics, there are more than 350,000 construction and maintenance painters, with that number expected to grow by 7% for the next 10 years. [32] Construction and maintenance painters remove old finishes and apply paints, stains, and coatings on interior and exterior structures to prevent corrosion. Most painters learn their trade on the job with no formal training. Painters have one of the highest rates of injuries and illnesses among all occupations. Paint dust emissions of respirable particles accounted for up to 400 tons a year and represented the ninth highest cause of diseases in the painting industry. [33] They have a higher-than-average incidence rate (196.7 per 10,000 workers)

of nonfatal occupational injuries/illness and an average of 25 days away from work, with exposures to harmful substances being the dominant non-physical hazard. [32] Occupational exposure as a painter has been proven to have carcinogenic effects on humans. [34] Painters have consistently shown significant excesses in lung cancer mortality in both smokers (95%CI: 1.21-1.51) and non-smokers (95%CI: 1.09-3.67). [35] Construction workers were more than twice as likely to have a lung disease or cancer. [36] The probability of COPD in painters increases to over 10% by the age of 55. [37] Painting is associated with rhinitis symptoms (95%CI: 1.1-5.2), asthma 95%CI: 1.4-16.1) and chronic bronchitis (95%CI: 1.0–8.4) when compared to carpentry work. [38] In a four-year study, 16.2% of painters who worked at Department of Energy sites had an abnormal chest x-ray, and 42.9% had an abnormal pulmonary function test. [34]

The current risk assessment process in health and safety focusing on pristine nanomaterials may not be appropriate to address possible risks of coatings with nanoparticles throughout the lifecycle of the product. In coatings, nanoparticles form agglomerates with polymers; however, the integrity of these agglomerates may be compromised by environmental and mechanical factors resulting in metals and metal oxides dislocation and release over time. [11,36] An important “end-of-life” exposure scenario that directly leads to the generation of respirable paint dust (particles with diameter less than 1.0 μm) is the mechanical abrasion (sanding) of coated surfaces. There have been few paint dust research papers published. Koponen et al. [6] found that the sanding dust of walls and wood coated with nano-containing products was dominated by particles in the 100-300 nm size range, and Gomez et al. [8] found that 80% of the collected paint dust particles had TiO_2 nanoparticles based on electron microscopy.

However, as of 2016, more than 80% of workers did not know if nanoparticles were even present at the worksite. [3] There is currently very little information regarding how prevalently nanoparticles are used in the construction industry. As of 2017, over 550 commercial grade construction products have listed the presence of nanoparticles. There is a lack of systematic investigation and understanding of the parameters affecting the release and their physicochemical properties.

REGULATORY FRAMEWORK

Paint dust regulations are governed by the Occupational Safety and Health Administration (OSHA). Most nanoparticle filled aerosol exposure is bracketed under unregulated particulates which lets workers be exposed to nanoparticle filled dust at a time weighted average (TWA) permissible exposure limit (PEL) of 15mg/m^3 for total particle mass and 5mg/m^3 for the respirable fraction. [39] At the time of writing the National Institute of Occupational Health and Safety (NIOSH) has set no enforceable limits for agglomerated or pristine nanoparticles. OSHA, however, has set a recommended exposure limit (REL) for carbon nanotubes and TiO2 of 0.3 mg/m^3 using recommendations from NIOSH studies. [42]

With ENMs it is hard to determine a safe occupational exposure limit (OEL). There have been several studies covering the nanoparticles in construction while proposing OELs. The range of the proposals for the TiO_2 OEL ranged from 0.017mg/m^3 to 5mg/m^3. [42] This large range, with the upper boundary being the minimum for the PEL of unregulated particulates as well as having a large portion of the range under the REL, highlights the concerns for better regulation and oversight for ENMs.

PERSONAL PROTECTIVE EQUIPMENT

Inhalation is the predominant route of exposure, followed by dermal absorption to a much lesser extent. [34] Personal respirators are one of the more commonly used devices in protection against inhalation. The efficiency of respirator filters relies on the filter material, and on pre-charging of the filter fibers. The fibers are made from a type of nonwoven material, usually polypropylene or cellulose, depending on manufacturer. Charging the filter fibers helps protect against particles above 0.3 microns and raises the penetration (P_m), the percentage of particle count that makes it through the filter.

$$P_m = \frac{C_{out}}{C_{in}} \quad \text{Eq. 1}$$

Filter performance, and the number of particles that can make it through them, is based upon the four main metrics of the filter. These are the fiber diameter, pore size, filter thickness, and the solidity of the filter. The fiber diameter is the size of the individual fibers that make up a fibrous filter, which is what most respirators are. The smaller the fiber the closer together they can be, while still leaving gaps for air to pass through. Pore size is the size of the holes in the filter. These holes are how the filter works, by letting air pass through the filter in such a way that the contaminants in the air can be removed. The pore size is a large indicator on how much particulate is captured by the fibers. Filter thickness defines how many layers of fibers that the travelling air must go through. If the filter is thick enough, only a negligible number of particles can make it through no matter the size of the particle. However, this makes using the respirator in a work setting harder due to stress placed on the worker trying to breathe. At a certain point, the filter will be so full of particulates that the act of breathing through the

respirator will not be easy enough to continue using the mask. The usual amount of time that is recommended to wear a respirator before replacing it is 8 hours due to pressure drop. Solidity is how tightly the filter fibers are packed. It is the ratio of air versus fiber that makes up the whole filter. [40] Other key elements for determining filter usefulness are face velocity and the quality factor. The face velocity is the rate of air flowing through the filter. This is determined by the activities and breathing of the respirator wearer. The filter quality factor is determined through pressure drop and P_m. A good respirator has both low pressure drop and low P_m.

PERSONAL RESPIRATORS

The respirators we are focused on for the basis of this study is the N95 (i.e. when subjected to careful testing, the respirator blocks at least 95 percent of very small (0.3 micron) test particles) The filter used in an N95 is usually a four layered system with the outer layer made of nonwoven electro spun polypropylene, a middle layer of filter which is commonly either cellulose or polyester, a second middle layer of melt-blown polypropylene, and another outer layer of nonwoven, electro spun polypropylene. The entire filter system is encapsulated inside a protective material, reducing the risk of filter materials escaping into the user's airway. Respirator filters have been electrostatically charged to help with particle removal. The mix of materials and production methods were designed to reduce the weak points of the filter.

Melt-blown filters have a smaller porosity than the electro spun filter of the same material. However, it has a higher penetration rate. In some studies, the penetration rate of melt-blown polypropylene had a penetration percentage of close to 40% for particles

between 50 and 100 nanometers at 5400 liters per hour (L/h) airflow, which correlates to 90 LPM. Respirators are tested for use at 85 liters per minute of airflow, which corresponds to a 9.44 cm/s face velocity, the NIOSH standard. [27] The consensus is that the melt-blown fibers have too much non-uniformity. Channels may occur in the product, allowing for a smaller particle's P_m. Also, the increase of airflow in increments of 900 L/h (15 LPM) showed significant increases in penetration percentage. The protection layers in the nano range must be from the electro spun filter with the higher porosity. The same studies show a styrene copolymer electro spun filter have less than 2% penetration at 90 LPM. It follows that materials tests of the filter at 85 LPM would be well within the 5% P_m allowed for the N95. Seeing as field tests have shown a higher P_m, the possibility of materials with higher porosity and not the traditional electro spun nonwoven plastic-based filters were investigated for ways to improve total overall N95 efficiency for field environments.

There is an inherit fault in the N95 protection when it comes to nanoparticles. Multiple studies have shown that there is a weakness in the respirator's prevention ability in the above 20nm range. A recent pilot study has also shown that the P_m of particles with diameter between 27.4 - 86.5nm through N95 respirators may exceed 5%. [41] The study showed P_m rates could be as high as 0.54. These findings are either a little higher or consistent with filtration efficiency of fiber filters. Fiber filters have demonstrated a decline in efficiency for particles in the range of 50-100 nms. [40] The P_m in this range has been demonstrated to be statistically higher compared to much smaller or larger particles when the respirators were challenged with particles ranging from 20-1000 nanometers. [42] The same study showed that the most penetrating particle size (MPPS)

for the N95, as well as other respirators, was approximately 50 nanometers. These filter deficiencies can be enhanced when dealing with face velocities outside the normal range. Some nano sized particles have a higher P_m at face velocities above 5cm/s. However, NIOSH has stated that their testing does not consider particles under 100 nanometers. Their own testing has shown that particles between 30-100 nanometers have shown higher penetration rates in charged filter media, the kind used in most commercial respirators. An older study had presented data with the P_m of N95s below 100 nanometers to be less than five present for all tested nano sized particles, however, 82 percent of all particles that passed through the respirators were smaller than 90 nanometers. [41] This aligns closely with Balazy et. al [43] when they demonstrated that pre-charged fiber filters have the poorest protection from particles between 35-70 nanometers.

FILTRATION

The capture of particles by a filter is achieved through five mechanisms, namely, (i) interception, (ii) inertial impaction, (iii) diffusion, (iv) gravitational settling, and (v) electrostatic attraction. [40] The first four mechanisms are identified as mechanical mechanisms. The total filter efficiency is the sum of all the mechanical deposition mechanisms.

$$E_{\Sigma} = E_R + E_I + E_D + E_G \qquad \text{Eq.2}$$

Where E_R, E_I, E_D and E_G are the filtration efficiency by interception, inertial impaction, diffusion, and gravitational settling, respectively. Electrostatic attraction is used to raise filter efficiency without adding anything else to the filter. However, it is

difficult to determine exactly how much the efficiency is increased by, for the individual particle charge must be known as well as the charge of the fibers.

Interception is when the particle, following its path on the airstream, is brought within one particle radius of a fiber in a filter. This leads to capture of the particle by the fiber. Interception efficiency is related to fiber diameter of the filter. The single-fiber efficiency (E_R) for interception (Eq. 3) depends on the ratio (R) of particle diameter (d_p) to filter fiber diameter, (d_f), the filter solidity (α) (i.e., how densely packed the fibers are in a filter) and Kuwabara constant (Ku) (Eq. 5). Interception helps more in the particle size ranges with the lowest collection efficiency.

$$E_R = \frac{(1-\alpha)R^2}{Ku(1+R)} \quad \text{Eq.3}$$

$$R = \frac{d_p}{d_f} \quad \text{Eq.4}$$

$$\text{Ku} = -\frac{ln\alpha}{2} - \frac{3}{4} + \alpha - \frac{\alpha^2}{4} \quad \text{Eq.5}$$

Inertial impaction is for when the particle in the airstream is too big for the airflow to keep it contained. When the airstream changes direction, the particle does not follow, and impacts upon the object the airstream was flowing around. Impaction affects larger particles much more than smaller particles and starts having an effect on filtration on particles slightly larger than 0.1μm. The single-fiber efficiency of impaction is determined by Stokes number (Stk), which is a ratio of the particle relaxation time versus the time it takes for the particle to navigate around an obstacle. The equation also involves the diffusion flux (J), which is a function of α and R.

$$\text{Stk} = \frac{\rho_p {d_p}^2 C_c U_0}{18 \eta d_f} \quad \text{Eq. 6}$$

$$J = (29.6 - 28\alpha^{0.62})R^2 - 27.5R^{2.8} \quad \text{Eq. 7}$$

$$E_I = \frac{(Stk)J}{2Ku^2} \quad \text{Eq.8}$$

Diffusion is when the particles are small enough that Brownian motion gives them a probability of moving enough outside of the air stream to interact with a filter fiber. The particles are so light that the air stream they are in does not fully affect them, and they drift about as they move in the direction of the air flow. Diffusion is a large part of the elimination of particles by filtration under 100nm. Diffusion efficiency is determined by the Peclet (Pe) number which is a function of the face velocity (U_0), the velocity of the air stream over the face of the filter. Diffusion is the most useful mechanism for removal of particles under 500nms. It is the only filtration mechanism that actually improves as the size of the particle decreases.

$$\text{Pe} = \frac{d_f U_0}{D} \quad \text{Eq. 9}$$

$$E_D = 2Pe^{-0.66} \quad \text{Eq. 10}$$

Gravitational settling deals with larger particles. The force of gravity effects the larger particles more, causing particles above 1.0µm to be greatly affected by settling. Particles under 100nm are not heavily impacted by gravitational settling. The equation for settling is an approximate and depends on the direction the filter is facing in relation to the air stream and gravity. In our experimental set up, the air stream was the opposite of the V_{ts} or terminal settling velocity. This makes the equation for the filter efficiency due to gravity:

$$G=\frac{\rho_g {d_p}^2 C_C g}{18\eta U_0} \quad \text{Eq.11}$$

$$E_G \approx -G(1+R) \quad \text{Eq. 12}$$

Electrostatic attraction is the use of creating a charge in the filter fibers. This charge will draw opposing charged particles, as well as neutral particles. The electrostatic attraction in filter fiber is usually created by using plastic fibers and corona charging them to get a semi-permanent charge, with one side positive and the other negative. This is one of the reasons that N95s have a shelf life as the charge will fade over time. The mathematical percentage for penetration at ~0.11μm is greater than 20%. Since this is not the actual case for most filters, it stands that the reduction in penetration is created by electrostatic attraction. Lathrace et al. [44] determined that the drop from a respirators MPPS from greater than 300 nanometers to less than 100 nanometers is due to the electrostatic charge. While this drastic change in the MPPS is due to charging, the introduction of electrostatic charge is helpful at most size ranges of particles. The equation for electrostatic attraction incorporates the dielectric constant (ε_f), the charge of the fiber (q), and the permittivity of a vacuum (ϵ_0). The major driving function for this mechanism is the fiber charge and face velocity.

$$E_q = \left(\frac{(\varepsilon_f - 1)}{(\varepsilon_f + 1)} \frac{q^2}{12\pi^2 \eta U_0 \epsilon_0 d_p d_f^2}\right)^{0.5} \quad \text{Eq. 13}$$

OBJECTIVES

This work is focused on the N95 respirator and modifications possible to raise the collection efficiency in the nanoparticle size range. The work initially investigated the production of TiO_2 at the nanoparticle size range in a work environment due specifically to the abrasion of paint that had nano sized TiO_2 within. The focus was specifically geared for particles under 300 nanometers and the possibility of exposure to particles of that size. This dissertation provides an analysis of sanding of freshly painted nanoparticle infused paint, as well as weathered samples of the same paint, which led to the testing and verification of possible modifications to the N95 respirator. The specific aims of this study include:

1. Characterize the physicochemical and morphological aspects of paint dust created through abrasion of paint containing nano sized TiO_2 particles within.
2. Characterize the effects that environmental weathering and exposure have on paint dust emissions during the abrasion process.
3. Create and assess filter combinations and media that can decrease filter penetration of TiO_2-embedded paint dust nanomaterials.

This work initially focuses on the risk assessment to construction painters during the abrasion process of paint containing nanoparticles as both a pristine coating of paint and a weathered version of the same paint. After the risk assessment confirmed a possibility of exposure to free and exposed nanoparticles, work was then performed to lower that exposure risk. The information in this dissertation can help contribute to greater protection for construction workers in other fields, as well as lead to more robust risk assessments in a growing field.

EXPERIMENTAL

Materials

A commercially available latex paint and primer formulation for indoor surfaces was purchased in bulk to be able to use the same batch for all studies and test conducted. Panels were bought all at once and consisted of Northern pine boards from one distributor.

Testing

Particle size and concentration

The aerosol size distribution was monitored using a suite of continuous particle sizers and counters that directly measure the aerodynamic diameter (d_a). These include the wide range particle spectrometer (WPS) (Model 1000XP, MSP Corp., Shoreview, MN) and the condensation particle counter (CPC) (Model 3771, TSI Inc., Shoreview, MN). Using the data, we determined the count median diameter (CMD) and geometric standard deviation (GSD). Using the CMD and GSD we determined the concentration of the particles at different size points and also determined the amount of mass generated for those size points.

Scanning Electron Microscopy (SEM)

We used an SEM (Quanta 650 FEG, Eindhoven, the Netherlands) at the UAB Scanning Electron Microscopy Laboratory to physically determine presence of nanoparticle TiO_2 as well as other components of the paint. All individual dust samples

were collected on filters and mounted on aluminum stubs. Imaging was done with no sputter coat at low vacuum at an accelerating voltage of 15 kV Determination of material makeup was done through the EDS function of the SEM.

Attenuated Total Reflectance Fourier Transform Infrared Spectroscopy (ATR-FTIR)

ATR-FTIR spectroscopy was used to reconcile the presence of wood and paint organic polymers in dust and changes in organic composition. ATR-FTIR spectra of paint dust samples were measured using an ALPHA spectrometer (Bruker Corp., Billerica, MA) equipped with a single reflection diamond ATR in the UAB chemistry department.

Inductively coupled plasma mass spectrometry (ICPMS)

ICP-MS analysis was used to determine exact concentrations of elements found in the abrasion samples. The limit of detection varies from 0.001 to 5 µg/l for the target elements of Al, Si, Ti, Zn, Cu and Fe. The ICP-MS was done by a third party at the University of Arkansas at Fayetteville Stable Isotope Laboratory.

Quartz Crystal Microbalance (QCM) Cascade Impactor

The cascade impactor we used (PC-2, California Measurements, Inc., Sierra Madre, CA) was to determine total mass of particle sizes before and after the tested filters. Particle mass was the focus point as the nano sized particles produced many particles but the mass of larger, less plentiful particles have more of an effect on a person versus many particles that have infinitesimally smaller mass.

ORGANIZATION OF WORK

The work in this dissertation in arranged into three articles that are consistent with and work to answer the goals that are laid out in the objectives section. An introduction and literature review introduces the material of the thesis, and a general conclusions summarizes the body of work.

Article 1 details the design and construction of the CARES that is used in all three manuscripts. It characterizes the abrasion aerosol makeup both morphologically and physiochemically, building the argument that nano TiO_2 is a concern and work on improving the N95 is something that needs to happen. Article 2 determines the effects of weatherization and pollution on the TiO_2 NEPs that are used in the coatings industry. It determines when TiO_2 ENMs are more likely to break free from the NEPs during abrasion and end-of-life procedures. Article 3 details the many different filter media that are combined and tried with the N95 filter to help reduce the chance of TiO_2 getting into the construction painter's airway. It determines the correct combination of filters to raise the protection level for the worker.

CHARACTERIZATION OF PAINT DUST AEROSOL GENERATED FROM MECHANICAL ABRASION OF TIO_2-CONTAINING PAINTS

by

ADAM W. NORED, MARIE-CECILE G. CHALBOT AND ILIAS G. KAVOURAS

Journal of Occupational Hygiene 15(9), pp.629-640

Format adapted and errata corrected for dissertation

ABSTRACT

The purpose of the study was to determine the potential for release of titanium dioxide nanoparticles in paint dust. The coatings aerosol resuspension system was developed and used for testing the generation and physical, chemical and morphological properties of paint dust particles from mechanical abrasion (i.e. sanding) of coated wood surfaces. The paint dust emissions from bare and coated wood surfaces with multiple coatings using variable sandpaper grits were evaluated. Substantially higher particle number concentrations were measured for paint dust containing particles in the nano range (particles with aerodynamic diameter less than 100 nm) than those measured for wood dust. The variability of particle number concentration and size distribution of paint dust derived under different conditions indicated that considerable quantities of nanoparticles may be released from mechanical abrasion of painted surfaces that may induce unhealthy exposure conditions. Moreover, spectroscopic and microscopic analysis identified the presence of paint and wood components in paint dust, including titanium dioxide agglomerates that were originally embedded in the paint. The agglomerates were mostly attached to particles with sizes < 100 nm enabling them to potentially penetrate into the lower respiratory tract. These results demonstrated that the paint dust exposure generation system can provide qualitative and quantitative information on particle emissions and the abundance of nanoparticles from paint sanding in realistic conditions and they may be used to assess occupational and environmental exposures and risks. Furthermore, the prevalence of titanium dioxide nanoparticles in paint dust highlights the potential for

exposures of painters and other occupational groups to hazardous paint dust and the need for protective devices and strategies aiming to reduce exposures to nanoparticles.

Key words: Nanoparticles, pigments, scanning electron microscopy, spectroscopy, sanding

INTRODUCTION

Metals and metal oxides nanoparticles (i.e. particles whose size, shape and chemical content are manufactured in the nano-scale) have been integrated as free powders, stabilized particles in suspensions or mixed into paint batches and granulates.[1] They improve the properties and functionality of paints such as coloring, integrity, thermal insulation, bactericidal activity, fire retardant and self-cleaning.[2-7] Those typically used in coatings include titanium dioxide (TiO_2), silicon dioxide (SiO_2), silver (Ag), zinc oxide (ZnO) and aluminum oxides (Al_2O_3).[8] Inhaled pristine nano-metals and metal oxides affect the lung, but are also cleared into circulatory systems, lymphatic system, nervous system, gastrointestinal tract and cross the blood/brain barrier.[9-13] They are shown to induce fibrosis, emphysema and tumors in the respiratory tract, lymphocytes damage, thrombosis, cardiovascular and neurodegenerative diseases.[14-18]

Construction and maintenance painting workers are exposed to a large variety of substances in paint and paint dust. There are at least 215,000 painters in this sector excluding part-time and undocumented workers who may comprise a significant fraction of the construction workforce.[19] Painters are occupationally exposed to known human carcinogens. [20] Painters have consistently shown significant excess in lung cancer mortality for both smokers (relative risk of 1.35 (95%CI: 1.21-1.51) and non-smokers (relative risk of 2.00 (95%CI: 1.09-3.67)).[21] They also have a higher than average incidence rate (235.9 per 10,000 workers; average of 104 per 10,000 workers) for nonfatal occupational injuries/illness and a median of nine (9) days away from work, with exposures to harmful substances being the dominant non-physical hazard.[22] Painting is

associated with rhinitis symptoms (odds ratio: 2.4, 95% CI: 1.1-5.2), asthma (odds ratio: 4.7, 95%CI: 1.4-16.1) and chronic bronchitis (odds ratio: 2.9, 95%CI: 1.0–8.4) when compared to carpentry work.[23]

The current occupational risk assessment process in occupational health and safety focusing on individual chemicals may not be appropriate to address possible health risks of paints with nanoparticles throughout the lifecycle of the product. In paints, nanoparticles form agglomerates with paint polymers; however, the integrity of these agglomerates may be compromised by environmental and mechanical factors resulting in metals and metal oxides dislocation and release over time.[24-27] An important *"end-of-life"* exposure scenario that directly leads to the generation of respirable paint dust is the mechanical abrasion (i.e. sanding) of painted surfaces. Koponen et al.[28] found that sanding dust of wall and wood coated with nano-containing products was dominated by particles in the 100-300 nm size range. Gomez et al.[29] found that 80% of the collected paint dust particles have TiO_2 and Ag nanoparticles based on electron microscopy. These studies raise concerns regarding the potential for exposures to nanoparticles currently incorporated in paints; there is a lack of systematic investigation and understanding of the parameters affecting the release and their physicochemical and morphological properties.

The aims of this study were to: (*i*) determine the number concentration and size distribution; (*ii*) characterize the elemental and organic composition; and (*iii*) assess the presence of TiO_2, in released particles generated by the mechanical abrasion on painted wood surfaces with TiO_2-containing paint for different painting and mechanical abrasion conditions. For this purpose, a coating aerosol generation system has been developed to realistically simulate the generation of paint dust during sanding including commercially

available wood surfaces, paints, sanders and sandpapers typically used by painters in the construction industry. Paint dust samples were collected and their morphology and chemical content were determined by scanning electron microscopy (SEM), attenuated total reflectance Fourier-transformed infrared (ATR-FTIR) and inductively coupled plasma mass spectrometry (ICPMS).

METHODS

Paint Dust Generation

Fig. 1A shows the schematic diagram of the major components of the Coatings Aerosol Resuspension System (CARES). It is composed of a polyvinylchloride glovebox chamber (115 cm [L] x 60 cm [W] x 60 cm [H]) (Lancs Industries, Kirkland, WA) that is installed in laminar-flow ventilation hood (SG603 Model, Baker Co., Sanford, ME). Mechanical abrasion of the painted surface is done manually using an orbital sander. The inlets of the aerosol continuous monitors and integrated samplers are placed on the upper surface of the chamber, and about 40 cm above the working surface, to better simulate the distance between the wall and the painter's breathing zone. Fans on the side panels of the chamber ensured dispersion of particles. Additional air was introduced through a high-efficiency particulate filter (HEPA) to reduce the presence of background particles. Excess air is vented through filters to the ventilation hood. Particle number concentrations were continuously measured using DC1700 portable particle counters (Dylos Corp., Riverside, CA) inside the ventilation hood to ensure that particle background levels, before, during and after the experiments were kept low to eliminate potential contamination of paint dust measurements and for safety.

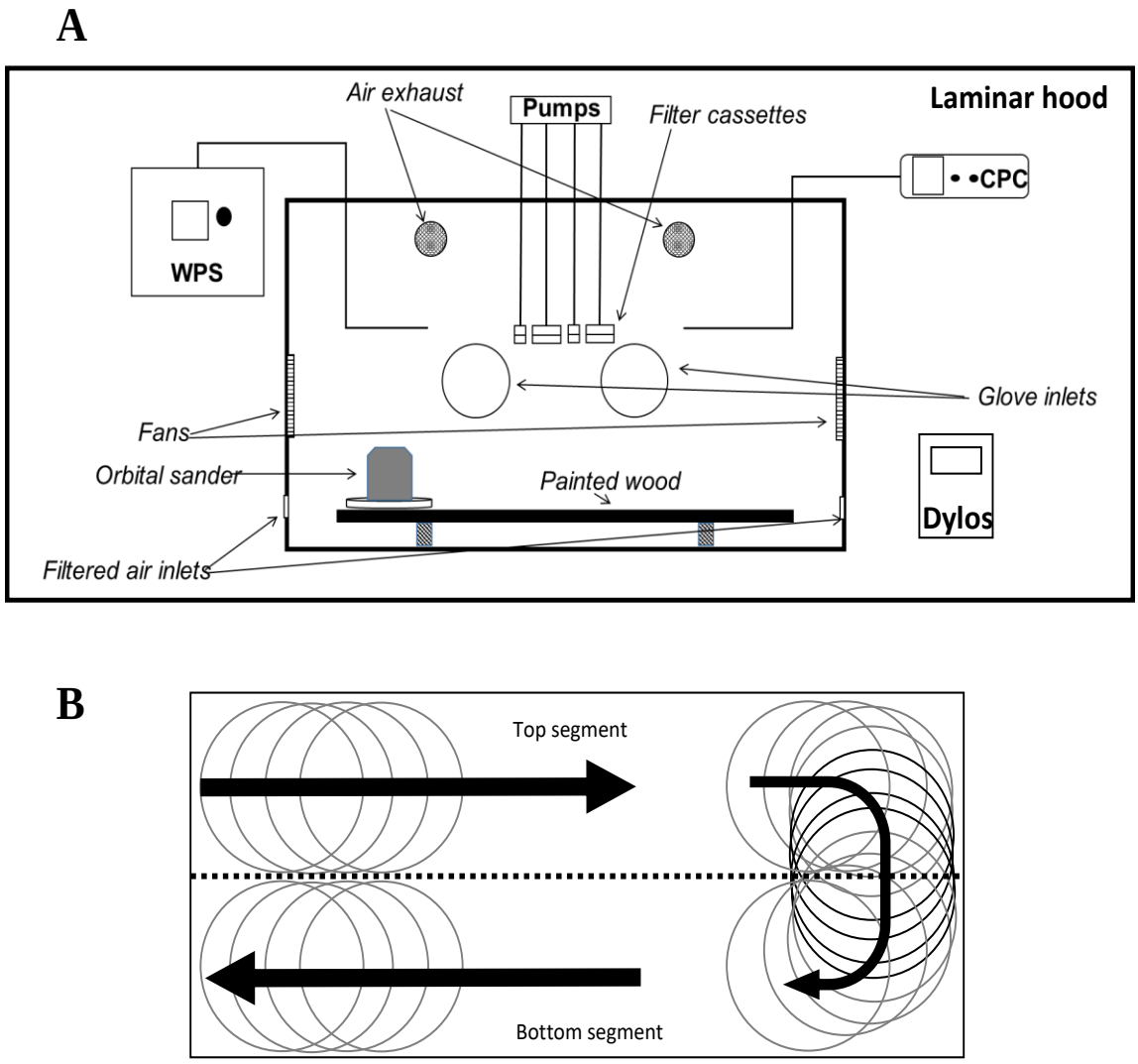

Figure 1. Schematic drawing (not-in-scale) of the Coatings Aerosol REsuspension System (CARES) (A). The painted surface is placed within the chamber and manually abraded with an orbital sander in a predetermined pattern (B). System specifications are given in Methods. The released dust is analyzed by real-time monitors and collected on appropriate substrates for chemical and morphological analysis.

The aerosol size distribution was monitored using a suite of continuous particle sizers and counters that directly measure the aerodynamic diameter (d_a). These include the wide particle spectrometer (WPS) (Model 1000XP, MSP Corp., Shoreview, MN) and the condensation particle counter (CPC) (Model 3771, TSI Inc., Shoreview, MN). The

WPS measured particles from 10 nm to 10 μm using differential mobility analyzer coupled with condensation particle counting (DMA/CPC) for particles with d_a < 0.4 μm (in 48 channels for 3 sec/channel) and optical light scattering (OLS) for particles with d_a > 0.4 μm (in 24 channels concurrently). The particle concentration ranges were up to 20 × 10^7 part/cm^3 for the DMA/CPC and 500 part/cm^3 for the OLS sensor. The CPC measured the total number of particles with d_a >10 nm. Particles in the sample stream are grown through the condensation of isopropanol vapors and counted using a single-particle-count mode. Paint and wood dust samples were collected on two sets of 13-mm cellulose filters and 47-mm Teflon filters (Pall Corp., Port Washington, NY) at 1.0 and 5.0 l/min flow rate, respectively, for subsequent SEM, ATR-FTIR and ICPMS analysis. . The 13-mm filters were selected to fit on SEM sample holder. The Teflon filters were selected to facilitate gravimetric, elemental and organic analysis (not shown here).

PAINTED SURFACE PREPARATION AND ABRASION

A commercially available latex paint and primer formulation for indoor surfaces was purchased. These paints are typically composed on pigments, fillers and binders in an aqueous suspension. According to the product's safety datasheet, the paint formulation was composed of water (49.6% w/w), non-volatile species (49.4% w/w), organic volatiles (0.9% w/w) and 2-amino-2-methyl-1-propanol (0.2% w/w) (CAS #: 124-68-5). It also included TiO_2 (3.2% w/w) (CAS #: 13463-67-7), crystalline silica (0.22% w/w) (CAS #: 14808-60-7) and cristobalite (0.11% w/w) (CAS #: 14464-46-1). Both sides of the wood panels (61.25 cm [L] x 28.75 cm [W]) were coated with two, four, six and eight paint coatings by using a 5-cm brush with 48 hours waiting periods between coatings. Six to

eight replicates were done for each sampling configuration. Panels were conditioned in a room (20^{o}C and 30% RH) for a week prior to sanding.

For abrasion, a BDERO600 2.4 Amp 5 inches (12.7 cm) orbital sander in its complete configuration (including the fitted filter) (Black & Decker, Towson, MD) fitted with Shopsmith® 5 inches (12.7 cm) aluminum oxide abrasive film discs (sandpaper, hereafter) (Shopsmith, Dayton, OH) was used. The sandpaper grits were 40, 120 and 220 (P_{40}, P_{120} and P_{220}, hereafter) and correspond to "Step 1: Extreme removal", "Step 2: Moderate surface preparation" and "Step 3: Fine scuffing" in the wood preparation and polishing processes. Each wood panel was divided in two segments (Fig. 1B). The sander was manually moved on the top segment along its length for 2.5 minutes, then vertically to the bottom segment and along its path for another 2.5 minutes. The sanding duration for each segment was selected to match the time required by the WPS to perform two full scans for the entire particle size range (2 measurements x 144 sec/measurement + 15 seconds delay between measurements).A new sandpaper pad was used for each experiment. A set of wood panels underwent the same treatment (handling and sanding, except painting) to characterize the physicochemical and morphological properties of wood dust. All activities were performed by a doctoral research assistant to control reproducibility uncertainties associated with differences in operator's behavior. Breaks were scheduled between tests to perform background tests on instruments and experimental setup and reduce operator's fatigue and ergonomic hazards.

CHEMICAL AND MORPHOLOGICAL ANALYSIS

The 47-mm Teflon filters were analyzed by ICP-MS for Al, Si, Ti, Zn and K at the University of Arkansas at Fayetteville Stable Isotope Laboratory. Samples were digested in concentrated HF/HNO_3 mixtures. Following digestions, samples were evaporated to dryness and re-dissolved in 2 ml of HNO_3. Prior to analysis, the sample was diluted with ultrapure water and known quantities of internal standards were added. ATR-FTIR spectra of wood dust, paint, and paint dust samples were measured using an ALPHA spectrometer (Bruker Corp., Billerica, MA) equipped with a single reflection diamond ATR. The spectra were recorded in the range of 400–4000 cm^{-1} with a resolution of 2 cm^{-1} over 64 scans. The morphology of paint dust particles was visualized by SEM (Quanta 650 FEG, Eindhoven, The Netherlands) under low-vacuum at an accelerating voltage of 15 kV at the University of Alabama at Birmingham Scanning Electron Microscopy Laboratory. Prior to analysis, the samples were mounted on a stub and sputtered with Pt. The working distance of samples was set at 10 mm with an accelerating voltage of 15 kV and an aperture of 30 μm. Images were taken at 5000× magnification. Elemental compositions were examined using an energy-dispersive X-ray spectroscopy analyzer with 30 mm^2 Silicon Drift spectrometer. Energy dispersive spectroscopy (EDS) analyses were performed at a magnification of 5000×, corresponding to an analyzed surface of 50 μm [w] x 30 μm [h]. It is noteworthy that the d_a measured by the particle sizers described previously refers to the diameter of the spherical particle with a density of 1,000 kg/m^3 and the same settling velocity as the irregular particle, while SEM measurements refers to the actual physical size of the particle.

CALCULATIONS

The count median diameter (CMD) and geometric standard deviation (GSD) were computed by plotting the particle number cumulative fraction as a function of particle diameter for each sample. The particle mass concentration (m in μg/m^3) for thoracic (PM_{10}), fine ($PM_{2.5}$), accumulation-mode ($PM_{1.0}$) and nano-size ($PM_{0.1}$) particles were computed using the WPS data as follows:

$$PM_x = \left(\sum_{i=1}^{n} \frac{\pi \cdot d_{a,i}^3 \cdot \rho_p \cdot N_i}{6}\right) \cdot 10^9 \qquad (1)$$

where *x* is the PM fraction ($PM_{0.1}$, $PM_{1.0}$, $PM_{2.5}$ or PM_{10}), $d_{a,i}$ (in m) and N_i (in part/m^3) were the midpoint particle aerodynamic diameter and number concentration for *i*-channel, and ρ_p was the particle density of 1,000 kg/m^3 that is typical for carbon-rich particles. For PM_{10}, all WPS channels were used. The channels with mid-point d_a from 0.01 to 0.103 μm, to 1.09 μm and 2.29 μM were integrated for $PM_{0.1}$, $PM_{1.0}$ and $PM_{2.5}$ mass estimates. The mean particle CMD, GSD and number and mass concentrations were computed from all replicates for each test (n = 6 – 8).

Particle number concentrations (PNC) were log-transformed and tested for normality using the Shapiro-Wilk test. The significance of difference in mean PNC values between groups was examined with the non-parametric Mann-Whitney (when two groups where compared) and Kruskal-Wallis (for more than two groups) tests at α=0.05. These tests were followed by Tukey's Honestly Significant Difference test. All analyses were done using SPSS (Version 23) (IBM Analytics, Armonk, NY) and Origin Pro (version 9.1) (OriginLab, Northampton, MA).

RESULTS

Particle Concentrations and Size Distribution

The panel A in Fig. 2 illustrates the PNC of wood and paint dust (two paint coatings) generated by the sander for approximately five (5) minutes using different sandpaper grits. The panel B in Fig. 2 shows paint dust PNS for multiple paint coatings using the P_{120} sandpaper. The mean (± standard error of the mean) PNC in paint dust varied from 147,000 ± 1,500 part/cm^3 for the P_{40} sandpaper to 235,000± 2,200 part/cm^3 for the P_{120} sandpaper and 278,000 ± 2,300 part/cm^3 for the P_{220} sandpaper. They were consistently higher than the wood dust PNC (83,000 ± 1,100 part/cm^3) using the P_{120} sandpaper (differences were statistically significant at the 95% level).

Paint dust PNC followed a multimodal pattern as the orbital sander moved along the painted surfaces (segment #1 in Fig.2A). The trends were more pronounced for paint dust generated using the P_{40} sandpaper and to a lesser extent for P_{120} and P_{220} sandpapers. Wood dust showed very little temporal variability. For paint dust generated using the P_{40} sandpaper, the PNC at the end of this modal cycles were comparable to the PNC measured for wood dust (segment #2 in Fig. 2A). It is noteworthy that the paint was completely removed using the P_{40} sandpaper and only partially removed for P_{120} and P_{220} sandpapers were used (see Figure S1 in Supplemental Information).

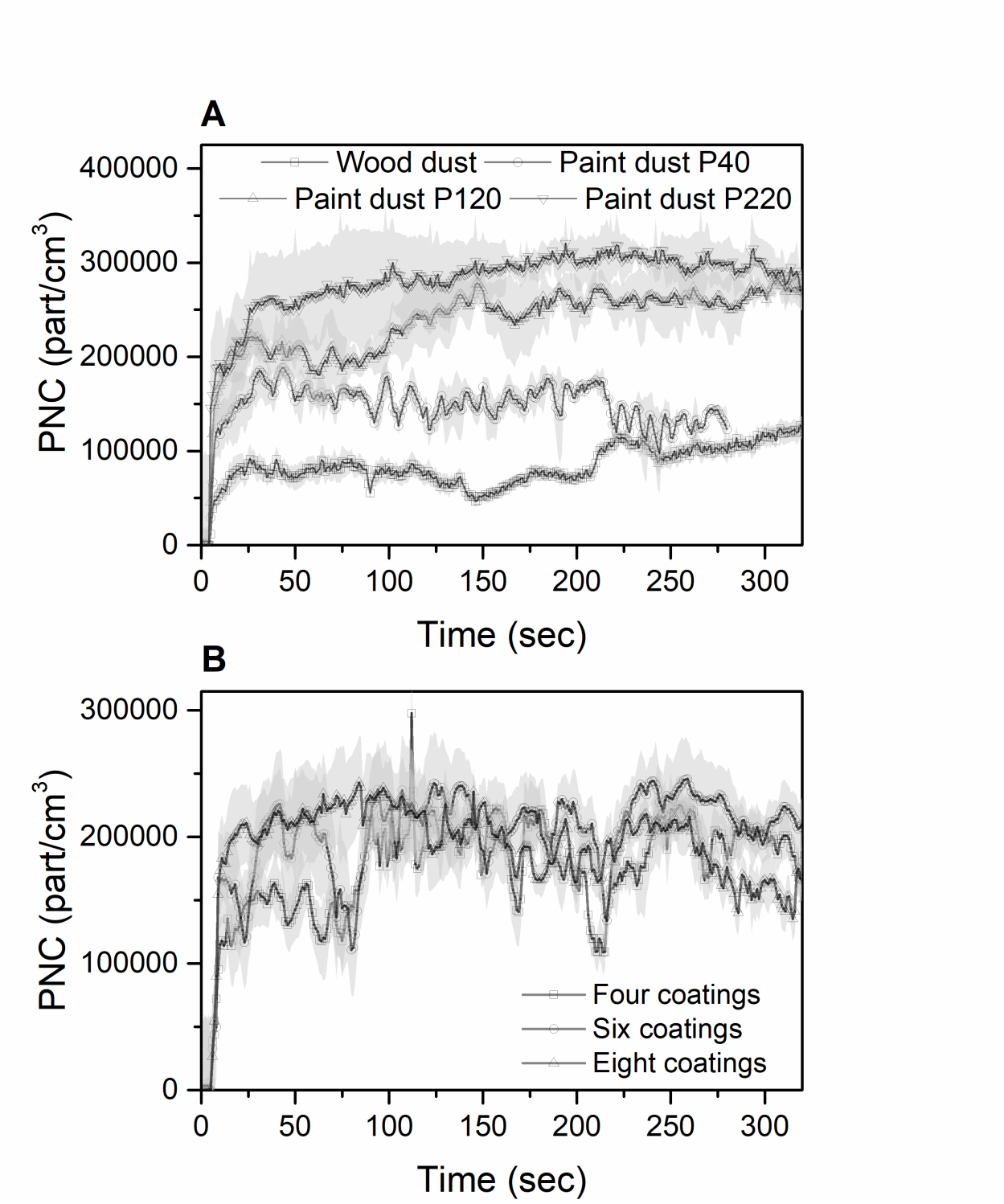

Figure 2. The particle number concentration of wood dust (with P_{120}) and paint dust with P_{40}, P_{120} and P_{220} sandpapers (A) and paint dust of four, six and eight coatings with P_{120} sandpaper (B) measured by the condensation particle counter.

The PNC of paint dust generated using the P_{120} sandpaper for wood panels with multiple paint coatings (i.e. four, six and eight) varied from 178,000 ± 2,000 part/cm^3 to 200,000 ± 2,000 part/cm^3) (Fig. 2B) (differences were also statistically significant at the 95% level). The multimodal PNC pattern over time was also observed for the multiple paint coatings. Its intensity (i.e. variability between maximum and minimum PNC) decreased as the coating layers increased. Note that paint was also inefficiently removed from panels with multiple coatings (see Figure S2 in Supplemental Information).

Figs 3A-D and 4A-C depict the normalized measured particle number and reconstructed mass (ca. Eq. 1 for each size range) size distributions of wood dust, paint dust using different sandpapers and for variable paint coatings. A one-mode distribution with maxima in the nano size range (d_a < 100 nm) was observed for paint dust particle number generated by different sandpapers and multiple paint coatings. The size distribution of particle mass reached a maximum in the coarse particle range (d_a > 2.5 μm). For paint dust generated by P_{120}, P_{220} and to a lesser extent for paint dust from multiple paint coatings, a second mode in particle mass distribution was observed in the accumulation mode (d_a < 1 μm) (see arrows in Figs 3C-D and 4B-C).

Table 1 presents the mean (± standard error) of the CMD, GSD and reconstructed PM_{10}, $PM_{2.5}$, $PM_{1.0}$ and $PM_{0.1}$ mass concentrations (ca. using Eq. 1). Paint dust was comprised of nano-size particles with a CMD of 35.6 – 39.4 (38.4 ± 1.6 nm for P_{40}, 39.4 ± 2.7 nm for P_{120} and 35.6 ± 2.2 nm for P_{220}). The CMD of wood dust (with P_{120} sandpaper) was comparable (31.0 ± 5.4 nm). The GSDs of paint dust particles were also similar for paint dust generated with the different sandpapers (2.4 ± 0.1 for P_{40} and 2.2 ± 0.1 for P_{120} and P_{220}), while a slightly higher GSD was computed for wood dust (2.8 ±

0.1) suggesting that larger particles may be present in wood dust. This was in agreement with the higher mass median diameter (MMD) (679 ± nm) and diameter of the mean mass (d_{mm}) (1,135 ± 204 nm) of wood dust as compared to those computed for paint dusts (MMD: 229 ± 38 to 356 ± 41 nm; d_{mm}: 308 ± 42 to 515 ± 60 nm). Comparable CMD (from 27.2 ± 1.5 to 35.5 ± 2.4) and GSD (from 2.2 ± 0.1 to 2.4 ± 0.1) (Table 1) values were calculated for paint dust generated using the P_{120} sandpaper on wood surfaces covered with multiple paint coatings.

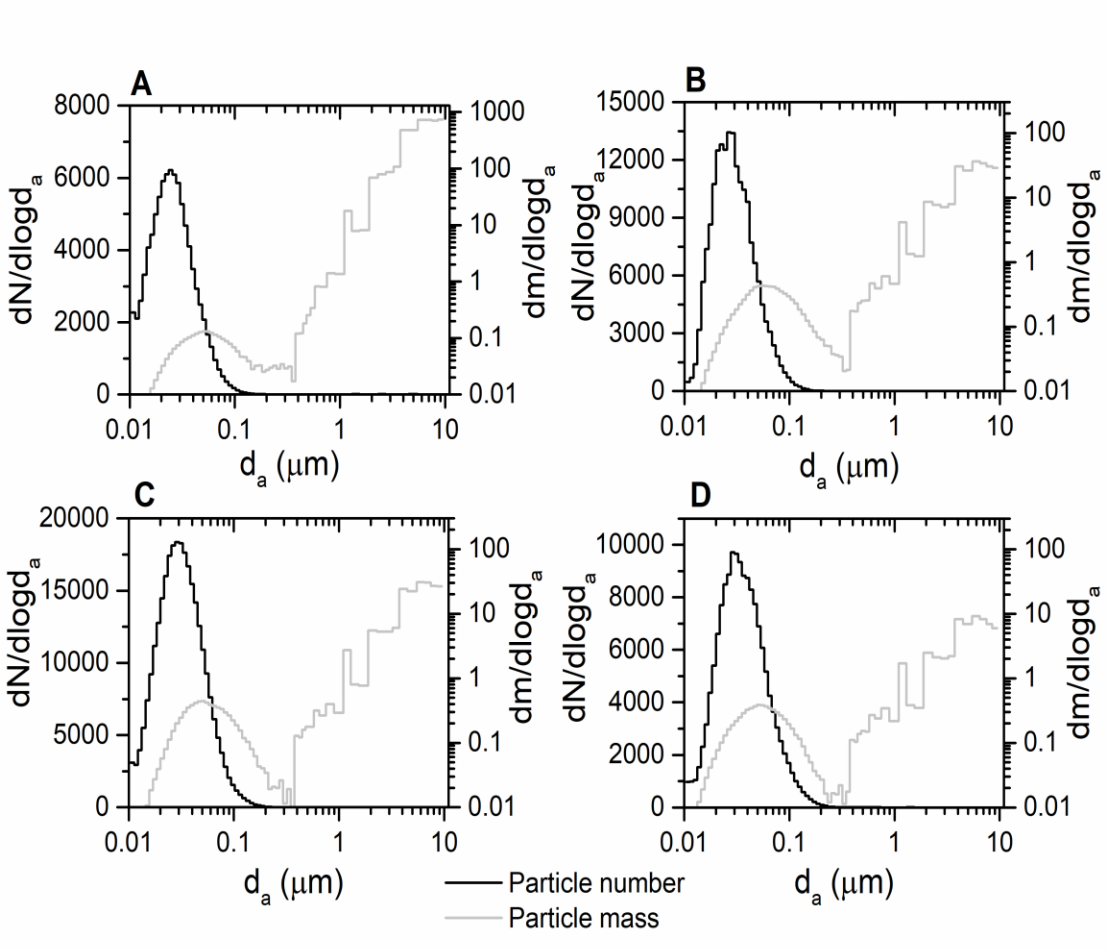

Figure 3. Particle number and mass (in logarithmic scale) size distribution of wood (A) and paint dust with P_{40} (B), P_{120} (C) and P_{220} (D) sandpapers

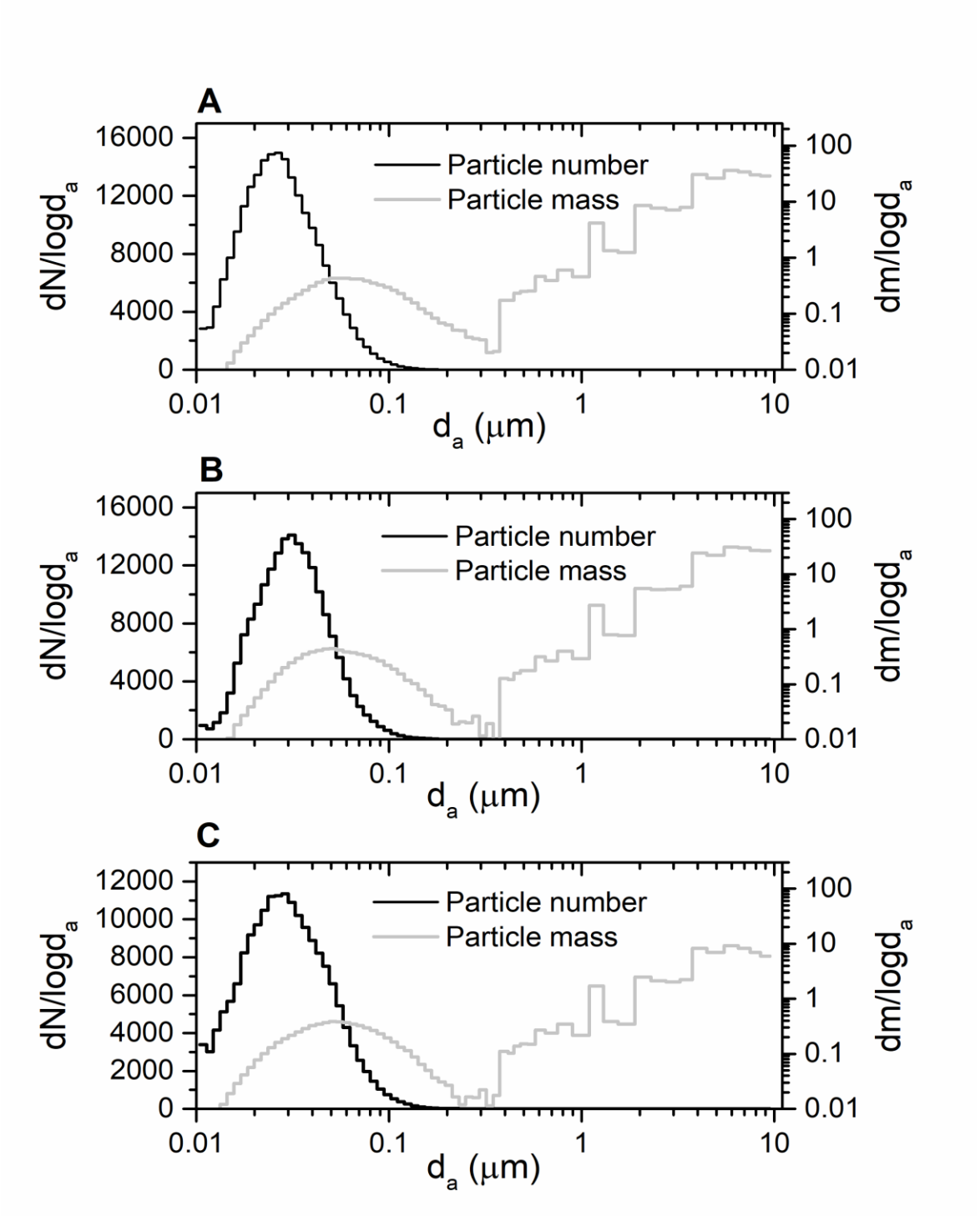

Figure 4. Particle number and mass (in logarithmic scale) size distribution of paint dust of four (A), six (B) and eight (C) coatings with P_{120} sandpaper

Table 1 Paint dust aerosol size characteristics and mass concentrations (mean ± standard error)

	Wood dust		**Paint dust**				
Sandpaper	P_{120}	P_{40}	P_{120}	P_{220}	P_{120}	P_{120}	P_{120}
Paint coatings	-	*2*	*2*	*2*	*4*	*6*	*8*
CMD (nm)	31 ± 5.4	38.4 ± 1.6	39.4 ± 2.7	35.6 ± 2.2	28.5 ± 1.9	35.5 ± 2.4	27.2 ± 1.5
GSD	2.8 ± 0.1	2.4 ± 0.1	2.2 ± 0.1	2.2 ± 0.1	2.4 ± 0.1	2.2 ± 0.1	2.3 ± 0.1
MMD (nm)	679 ± 122	356 ± 41	269 ± 41	230 ± 40	284 ± 34	229 ± 38	284 ± 30
d_{mm} (nm)	1135 ± 204	515 ± 60	370 ± 56	314 ± 54	416 ± 50	313 ± 53	308 ± 42
			Particle mass[A] (μg/m^3)				
TSP	16,222 ± 1,074	5,582 ± 1,386	1,113 ± 442	329 ± 35	864 ± 503	729 ± 428	229 ± 44
$PM_{0.1}$	3 ± 1	7 ± 2	17 ± 3	12 ± 3	9 ± 1	9 ± 1	8 ± 1
PM_1	16 ± 1	25 ± 2	36 ± 5	32 ± 15	20 ± 3	17 ± 2	15 ± 1
$PM_{2.5}$	359 ± 37	269 ± 65	94 ± 21	49 ± 15	72 ± 29	50 ± 20	31 ± 3

[A] Assuming spherical particles with a density of 1,000 kg/m^3

Assuming spherical particles with density of ρ_p=1,000 kg/m^3 (i.e. typical for carbon–rich aerosol), the reconstructed mean (± standard error) PM_{10} mass concentration of wood dust was 16.2 mg/m^3. It was substantially higher than the reconstructed PM_{10} mass concentration for paint dust using the three sandpapers. The paint dust PM_{10} concentration increased from 329 ± 35 to 5,582 ± 1,386 μg/m^3 as the sandpaper grit size decreased (from ultrafine to coarse sandpapers). For wood dust, the vast majority of PM_{10} mass were coarse particles (~98%), and only one-thousandth (or 16 ± 1 μg/m^3) was associated with the finer particles ($PM_{1.0}$) and one tenth of that was in the nano size ($PM_{0.1}$) range (3 ± 1 μg/m^3).

Approximately 5 to 15% of paint dust of PM_{10} was associated with the respirable fraction ($PM_{2.5}$) (269 ± 65 μg/m^3 for P_{40}, 94 ± 21 μg/m^3 for P_{120} and 49 ± 15 μg/m^3 for P_{220}). The $PM_{1.0}$ fractions accounted for 10%, 30% and 55% of $PM_{2.5}$ paint dust generated with P_{40}, P_{120} and P_{220} sandpapers, with 25-50% of them being in the nano size range, resulting in $PM_{0.1}$ mass concentrations as high as 17 ± 3 μg/m^3. The paint dust PM_{10} mass concentrations decreased from 869 ± 503 μg/m^3 to 229 ± 44 μg/m^3 as the number of applied paint coatings increased from four to eight, albeit around 10% was associated with the fine fraction. The $PM_{1.0}$ fraction account for 25 to 50% of $PM_{2.5}$, with more than 50% of $PM_{1.0}$ particles being in the $PM_{0.1}$ size range.

Paint Dust Composition

Chemical Analysis

The ATR-FTIR absorbance spectra of wood and paint are depicted in Fig. 5A. The spectrum of wood dust demonstrated unique absorption bands including stretching

O-H in-plane absorption bands in the 3200-3700 cm^{-1} typical in cellulose and polysaccharides. Other major absorption bands were attributed as follows: 2800 – 3000 cm^{-1} to C-H stretching, 1510 cm^{-1} to C=C stretching of the aromatic ring of lignin, 1465 cm^{-1} to C-H deformation in lignin, 1375 cm^{-1} to C-H deformation in polysaccharides, 1335 cm^{-1} to bending in-plane O-H, 1240 cm^{-1} to C-O stretch in lignin and broad band in 1024 cm^{-1} to C-O stretch in C-O-C cellulosic bridges.

The main absorption bands observed in the ATR-FTIR spectrum of paint were: 2800 – 3000 cm^{-1} (stretching vibration of the $–CH_2-$ group), 1730 cm^{-1} (stretching of the C=O group), 1450 cm^{-1} , 1385 cm^{-1} (stretching of CH_3 groups) , 1240 cm^{-1} (stretching of =C-H groups), 1140 cm^{-1} (stretching of the C-O group), 840 cm^{-1} (bending vibration of the aromatic C-H group). The broad bands in 400 – 650 cm^{-1} region were assigned to TiO_2.

Figs. 5B and C show the ATR-FTIR spectra of paint dust generated with variable sandpapers and multiple coatings, respectively. Clear similarities among paint dust, paint and wood spectra can be detected, reflecting the presence of both paint and wood species in paint dust. All paint dust samples retained the absorption bands in the 400 – 650 cm^{-1} region, previously attributed to TiO_2. Per Beer-Lambert Law, the absorption is proportional to the concentration; thus, more TiO_2 may be associated with paint dust generated with P_{120}/P_{220} sandpapers as compared to P_{40} sandpaper, and for paint dust generated from six and eight coatings compared to four coatings. The relative abundance of paint and wood particles may be derived from the spectral profile in the 800 – 1300 cm^{-1} region (dotted rectangular in Figs 5.A-C) that includes C-O absorption bands for wood dust (cellulosic and lignin) and paint dust (oil-based binders).

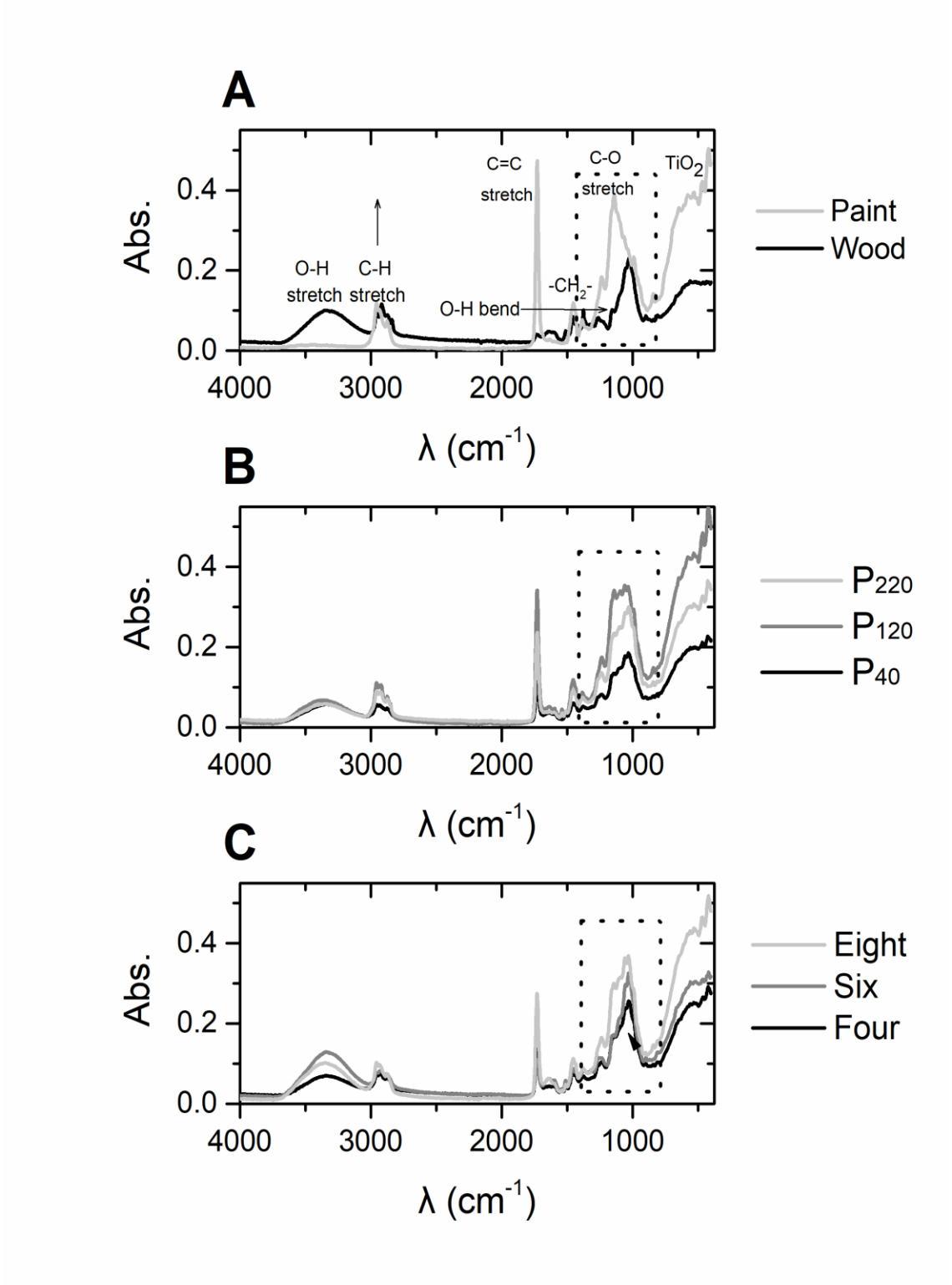

Figure 5. ATR-FTIR spectra of wood dust and paint (A), paint dust with P_{40}, P_{120} and P_{220} sandpapers (B) and four, six and eight coatings (C)

The relative contribution of paint species in paint dust increased as the sandpaper grit changed from P_{40} to P_{220} and the number of coatings increased. The prevalence of wood species also increased for different sandpapers but remained relatively unchanged for multiple coatings.

Figs. 6A-B show Ti concentrations in paint dust (in ng/mg of paint dust particles) and the Ti-to-Al ratios generated using three sandpaper types for multiple paint coatings measured by ICPMS. The measured levels of Ti, Al, Si, K and Zn are presented in Table S1. Paint dust Ti concentrations using the P_{120} sandpaper were comparable for all coatings (from 29 to 33 ng/mg of particles) but lower than those measured using the P_{40} (from 49 to 101 ng/mg of particles) and P_{220} (from 73 to 90 ng/mg of particles) sandpapers. Overall, Ti in the form of TiO_2, accounted for 0.01 to 0.02% by weight of total particle mass. Note that no size selective inlet was used, therefore TSP aerosol including large wood dust particles were collected. Assuming that TiO_2 particles may be present in the nano size range and that $PM_{0.1}$ particles accounted for approximately 1% of TSP by mass (Table 1), the relative abundance of TiO_2 may increase up to 2% by mass.

Aluminum (Al) was present in paint (see Figure 8 below) but can also be released from sandpaper. The Ti/Al ratio was used to assess the potential effect of sandpaper particles for different sandpapers and paint coatings. For wood panels with the same paint coatings (similar quantities of paint TiO_2), higher Ti/Al values indicated an enrichment of TiO_2 as compared to larger Al-containing particles in paint or sandpaper. In most of the experiments, the Ti/Al increased for coarse sandpapers suggesting the enhanced presence of paint particles as compared to those potentially released from sandpaper. In all cases, Al and Si concentrations added less than 1% to paint dust particle mass.

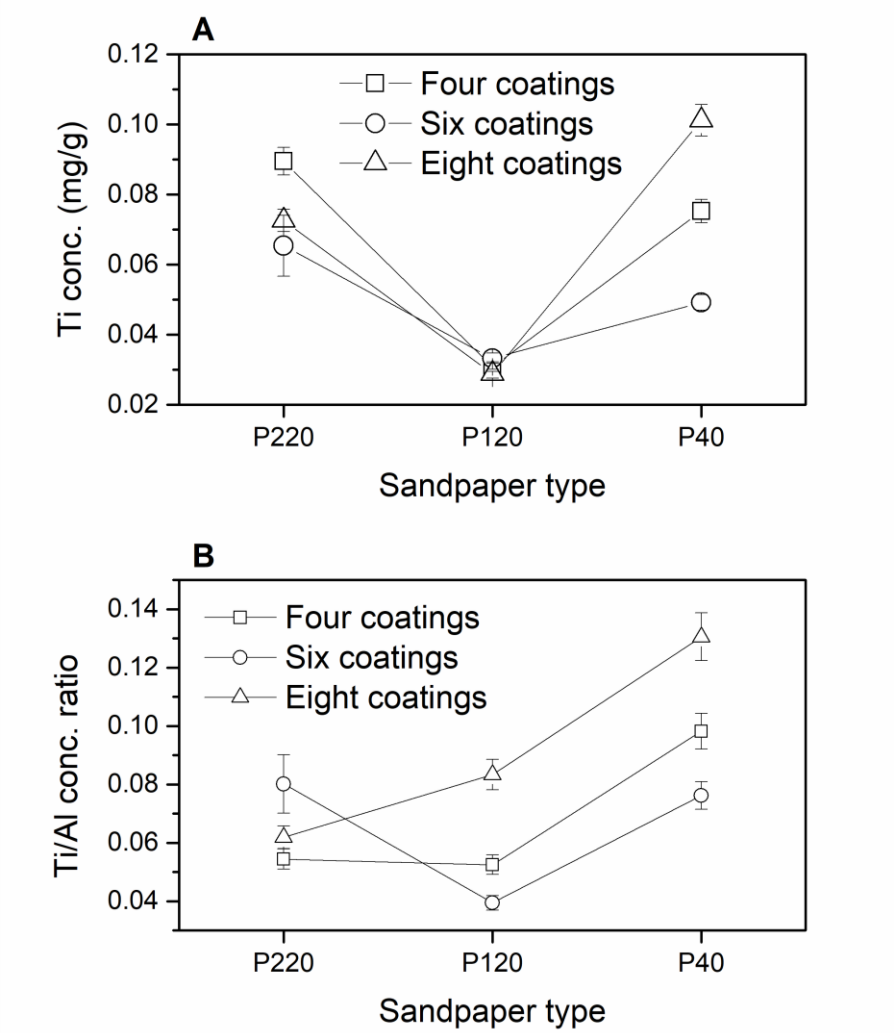

Figure 6. Particulate Ti levels (A) and Ti-to-Al concentration ratios for paint dust generated by sanding wood boards coated with multiple paint layers with different sandpapers.

Morphological Analysis

Fig. 7 depicts the SEM backscatter images of paint and paint dust generated by P_{120} with two coatings. SEM images of paint dust generated with different sandpapers and coatings are included in Supplemental Information (see Figures S3 and S4 in Supplemental Information). In backscatter SEM, carbon-based materials are projected in dark colors whereas metals are bright. The painted surface is characterized by a rather

uniform distribution of white spots that may be attributed to metal oxides. Released particles also contained TiO_2 nanomaterials in various shapes (spherical, amorphous) in the nano-size range (Fig. 7B and Fig. S5 in Supplemental Information). Larger fiber agglomerates were in the submicron range.

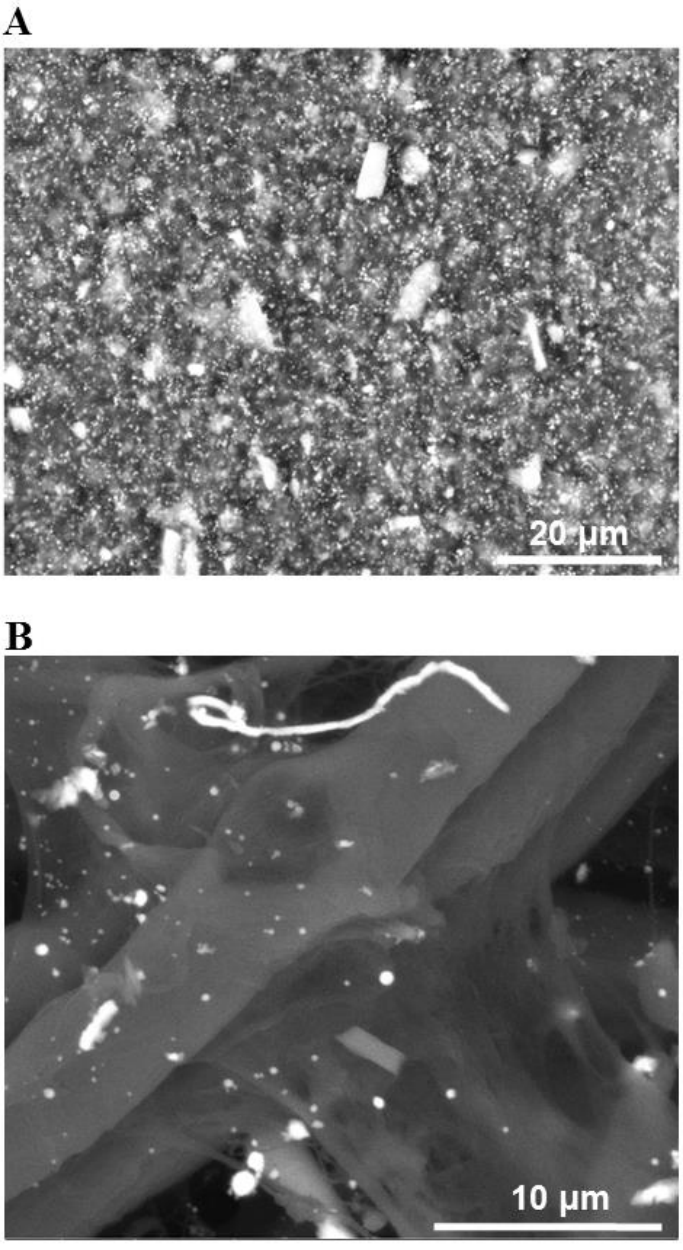

Figure 7. Backscatter SEM image of paint (A) and paint dust (B) (P_{120} sandpaper, and two coatings).

Figure 8 shows typical SEM-EDS spectra obtained from wood, paint and paint dust. Wood dust was entirely composed of C and O (ratio of 2:1). This is comparable to the compositional characteristics of wood, that is comprised of 80% of cellulose (represented as CH_2O, C:O=1) and 20% lignin (represented as $C_{10}H_{13}O_4$, C:O=5:2). No metals were observed in wood dust. In addition to C and O (ratios of 4:1 for paint and 1:1 for paint dust), paint and paint dust also comprised of Ti, Al, Si. Traces of Zn and K were observed in paint dust. The quantity of Ti was comparable in paint and paint dust (23 and 24%). The relative abundance of Si and Al increased from 12% and 7% in paint to 19% and 14% in paint dust, respectively. That may be suggestive of minor quantities of Al and Si particles released from the sandpaper. Note that C may also be associated with the filter material (cellulose).

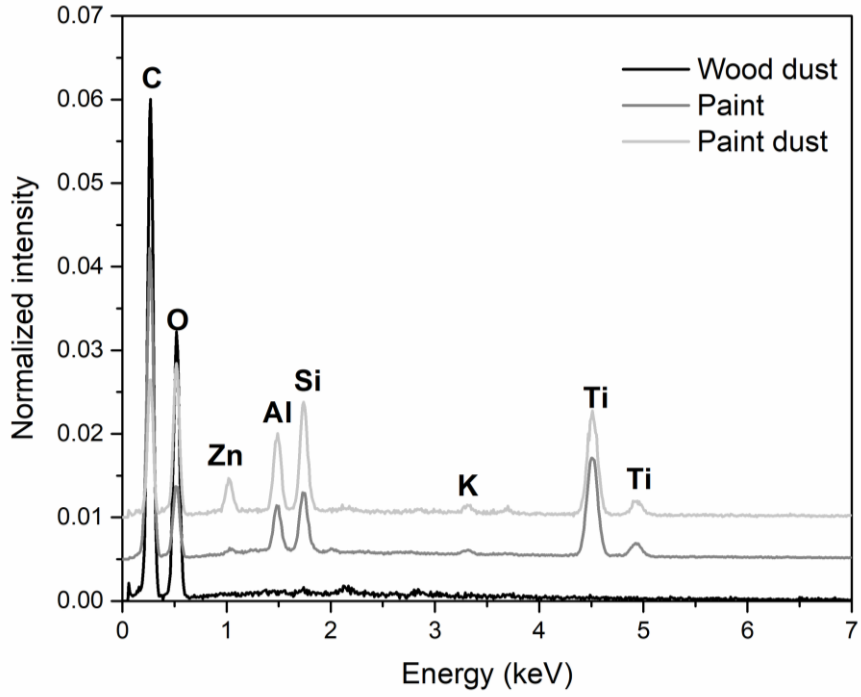

Figure 8. Typical SEM EDS spectra of individual particles in wood, paint and paint dust (P_{120} sandpaper, and two coatings).

DISCUSSION

The PNCs of dust generated from bare and painted wood surfaces with multiple paint coatings using different sandpapers have been monitored. Paint dust PNC was up to three times higher than wood dust PNC due to differences on wood and paint surface properties affecting particle generation.[30] Wood contains long fibers made of cellulose and lignin ranging from 30 - 300 μm in diameter and 10 μm - 4 mm in length.[31] On the other hand, painted surfaces are composed of single particles associated with pigments, filler particles in agglomerates with the polymeric binder, and other additives (e.g. thickeners, dispersants and defoamers) to achieve stability and application consistency. The type, size and quantity of pigments varied (TiO_2 for white and high opacity paint) but typical pigment particle sizes do not exceed 250 nm in diameter. Larger agglomerates may be in the submicron size range.[32] Paint dust PNC increased for finer sandpaper, which is consistent with the potential of particle in finer sandpapers to make chiseled scratches and dislocate smaller pieces of paint materials. On the other hand, coarse sandpaper has the capacity to remove larger quantities of material by generating larger particles, which was consistent with the particle size measurements and particle mass calculations. Another potential mechanism, albeit of minor importance for engineered metal-oxides nanoparticles, is the volatilization of paint organic polymers because of the heat developed on the surface by friction, and subsequent particle formation through condensation.

Previous studies have also found that engineered nanoparticles in wood sealants and coatings to protect against water and UV damage on plywood and hardwood panels may be released as agglomerates by mechanical abrasion.[33,34] Those studies however

found no significant differences in PNC between coated and uncoated surfaces. This may be due to differences on the thickness of coating materials (paint vs. sealants) and the type of wood panel. Plywood is made of thin wood layers patched, graded, glued and baked together, compromising the integrity/length of wood fibers, which may result in the generation of more nano-sized particles during sanding. It has been previously reported that nano-size particles may be generated by the orbital sander.[28] In this study, both measured paint and wood dust concentrations include sander-generated nanoparticles. As a result, even if all nano-size particles in wood dust were due to the sander, they could only account for up to 30% of paint dust nanoparticles. Previous studies suggested that submicron particles may also be generated by the degradation of sandpaper, as indicated by the presence of Si-Al particles.[28] Note that the average sandpaper particle diameters for P_{220}, P_{120} and P_{40} sandpapers were 68, 115 and 425 μm respectively.[33] In this study, SEM/EDS analysis indicated the presence of Al and Si in paint and paint dust, but not in wood dust generated using the same sandpapers. Elemental analysis by ICPMS showed that Al and Si particles accounted for less than 1% of particle mass. The prevalence of sandpaper Al particles may have decreased for coarse sandpapers.

Paint application of new wood surfaces in residencies and buildings typically includes one layer of primer, ultrafine sanding to smooth the wood surface, and two layers of paint. However, over time, more layers of paint may be applied without sanding. This may result in the accumulation of paint components including nanoparticles. No significant differences in PNC from surfaces coated with multiple paint layers were observed indicating that particle release rates under the same conditions (i.e. sandpaper

and sanding time) were comparable. However, more nano-size particles may be eventually re-suspended from multiple painted surfaces because more time would be required to effectively remove the accumulated paint.

Nano-size range particles were predominantly generated during abrasion of bare and painted wood surfaces. The CMD did not vary substantially (differences not significant at the 95%) for wood and paint dust generated by different sandpaper sizes. On the other hand, GSD differences among wood and paint dusts were statistically significant at the 95% level indicating that generation of nano-sized particles is favorable in painted surfaces. Wood dust was comprised of more coarse particles (with $d_a > 2.5$ μm) and less nano-size range particles (with $d_a < 100$ nm) compared to those measured for paint dust. As a result, more than 98% of wood particles by mass were not respirable. In comparison, on average 9.5% of paint dust particles by mass were respirable (from 1.8 to 14.9% for different sandpapers and coatings), with 20% of the respirable fraction being in the nano-size range (from 2.6 to 25.8% for different sandpapers and coatings). It is noteworthy that instantaneous particle size changes may not be entirely captured because of the WPS measurement method in which particle number concentration for different sizes is measured sequentially. This uncertainty may be more important as the sander moved on smoothed surfaces; however, the total PNC measured by WPS and average PNC measured by CPC for the same time period were comparable (percent of coefficient of variance (%CV) of less than 7%) indicating that there were no major particle size misclassification during the measurement period.

The types of the abraded surface and sandpaper modified the particle size range and their quantity (by number and mass concentration) but not the central tendency

indicators (CMD). The production of more nano-size paint particles may be related to the force energy required to break agglomerates of pigments, filler particles and other additives in paints as compared to large cellulosic/lignin fibers in wood. When paint is applied, its ingredients may adhere to the wood surface through mechanical interlocking, diffusion, adsorption and surface reaction and electrostatic interactions. More paint on wood surfaces (i.e. from painting over existing paints) may result in the release of more nano-size particles by mechanical abrasion because additional time would be required to efficiently remove all paint layers from the wood surface.

The release of paint materials included TiO_2 nanoparticles have been further confirmed by ATR-FTIR, SEM microscopy and ICPMS spectroscopy. Paint components accounted for the majority of organic and inorganic components in paint dust particles (no IR absorbance assigned to inorganic species was observed in wood dust). TiO_2 nanoparticles are found to be encapsulated or on the surface of nano-size paint particles and individually in different shapes and sizes mostly in the nano range. The relative abundance of TiO_2 on individual paint dust particles (as quantified by EDS detector in SEM) was comparable to that measured in paint. Compared to particle mass, TiO_2 nanoparticles accounted for 0.01-0.02% of TSP mass and up to 1-2% in the nano-size range. Albeit lower than the recommended NIOSH airborne exposure limit of 0.3 mg/m^3, the risk for adverse health effects through the inhalation of nano-size particles containing engineered nanoscale TiO_2 may not be discounted.

Previous studies showed that the toxicity of TiO_2 nanoparticles following 24-hr of exposure may be negligible compared to the toxicity of pristine TiO_2; however, the long-term effect (48-, 76- or 120-hours following exposure) was not examined. [34] Donaldson

et al. [35] demonstrated lung responses and distribution to other organs after 2 to 28 days following month-long exposures, indicating the persistence of TiO_2 nanoparticles. Encapsulated nanoparticles in agglomerates of water-based paint polymers in the submicron range (aerodynamic diameter (d_a) < 1 μm) can still penetrate into the alveolar region and upon decomposition, dissolution and/or uptake of the water-soluble polymer, they may be released intact in the lung or distributed in other organs maintaining their enhanced toxicity. The timing of TiO_2 release by dissolution of the paint polymers may also be important since nanoparticles can also translocate into the blood stream affecting other organs.

Currently, there are exposure limits for specific components integrated in paints (lead, chromium (VI)) but there are no exposure limits for paint dust or newer additives. The estimated total particle mass concentrations in this study were lower than the exposure threshold for wood dust (15 mg/m^3, note that wood dust TSP mass concentration exceeded the exposure threshold). However, the abundance of nano size particles is particularly worrisome (as high as 17 $\mu g/m^3$) as their estimated surface area may range from 4 to 23 cm^2/m^3. It is noteworthy that estimated particle mass exposures do not represent actual personal exposures because a smaller chamber (~0.5 m^3) as compared to a typical size room of 20-30 m^3 was used (may overestimate exposure estimates), albeit the ventilation hood was operating at 800 m^3/h flow rate leading to high air exchange rates in the CARES system (may dilute/underestimate exposure estimates). It has been previously shown doses of nano size particles substantially lower than those measured in this study may induce severe pulmonary toxicity and significant pulmonary inflammation and cytotoxicity potencies for TiO_2 doses as low as 0.0125 cm^2/cm^3.[36-38]

CONCLUSIONS

Metal and metal oxides nanoparticles have been integrated in paints and other construction materials because of their ability to improve their performance. Exposures to nanoparticles may be minimal assuming proper handling and use of the products, but little is known about the potential for exposures to nanoparticles at the end of paint's lifecycle which includes the removal of paint from surfaces by sanding. Our analysis clearly demonstrated the potential for the release of elevated particle concentrations. The majority of these particles were in the nano-size range accounting for up to 50% of respirable particulate matter. The nano-size particle number concentrations increased for finer sandpaper grits and more paint coatings; albeit lower particle mass concentrations were estimated. Chemical and morphological analysis determined that paint dust particles were comprised of a combination of paint and wood species including TiO_2 nanoparticles embedded in paint. They were found to be predominantly attached on the edge or inside particle agglomerates, albeit still in the nano-size range, therefore enabling the potential for penetration of nanoparticles containing nanoparticles in the lung alveoli and translocation in the blood.

The paint dust exposure generation system and use of commercially available equipment and supplies afforded the capability to simulate typical occupational conditions in a reproducible and traceable manner. Because of its modality, the generation system may be utilized to investigate a wide spectrum of exposure scenarios including paint and coating application by spraying. These findings call for further

research into the release of nanoparticles -embedded paint dust particles including the effect of the type and quantity of nanoparticles and the effect of weatherization. There is previous evidence that paint structural integrity deteriorates over time and nanoparticles may be released into the environment. Furthermore, in-vitro and in-vivo toxicological studies may provide significant insights on the biological effects of paint dust and the role of organic polymers and nanoparticles.

ACKNOWLEDGMENTS

The study was partially supported by the NIOSH funded Deep South Center for Occupational Health and Safety Education and Research Center (Award #: T42OH008436). The findings and conclusions in this report are those of the authors and do not necessarily represent the views of the National Institute for Occupational Safety and Health.

REFERENCES

1. Allen, N.S., M. Edge, A. Ortega et al: Degradation and stabilization of polymers and coatings: nano versus pigmentary titania particles. *Polym. Degrad. Stab*. *85*:927-946 (2004).
2. Carp, O., C. L. Huisman, and A. Reller: Photoinduced reactivity of titanium dioxide. *Prog. Solid State Chem*. *32*:33-177 (2004).
3. Sharma, V.K., R. A. Yngard, and Y. Lin: Silver nanoparticles: green synthesis and their antimicrobial activities. *Adv. Colloid Interfac.e 145*:83-96 (2009).
4. Gladis, F., A. Eggert, U. Karsten, and R. Schumann: Prevention of biofilm growth on man-made surfaces: evaluation of antialgal activity of two biocides and photocatalytic nanoparticles. *Biofouling. 26*:89-101 (2010).

5. Dallas, P., V. K. Sharma, and R. Zboril: Silver polymeric nanocomposites as advanced antimicrobial agents: classification, synthetic paths, applications, and perspectives. *Adv. Colloid Interface. 166*:119-135 (2011).

6. Holtz, R.D., B.A. Lima, A.G. Souza Filho, M. Brocchi M, and O.L. Alves: Nanostructured silver vanadate as a promising antibacterial additive to water-based paints. *Nanomed. Nanotechnol.. 8*:935-940 (2012).

7. Hanus, M.J., and A.T. Harris: Nanotechnology innovations for the construction industry. *Prog. Mater. Sci. 58*:1056-1102 (2013).

8. Schmid, K., and M. Riediker: Use of nanoparticles in Swiss industry: A targeted survey. *Environ. Sci. Technol. 42(7)*:2253–2260 (2008).

9. Hoet. P.H.M., I. Bruske-Hohlfeld, and O.V. Salata: Nanoparticles - known and unkown health risks. *J. Nanobiotechnol. 2*:12-27 (2004).

10. Oberdörster, G., E. Oberdörster, and J. Oberdörster: Nanotoxicology: an emerging discipline evolving from studies of ultrafine particles. *Environ. Health Perspect. 113*:823-839 (2005).

11. Liu, J., H.L. Wong, J. Moselhy, B. Bowen, X.Y. Wu, and M.R. Johnston MR: Targeting colloidal particulates to thoracic lymph nodes. *Lung Cancer. 51*:377-386 (2006).

12. Oberdorster, G., Z. Sharp, V. Atudorei et al: Translocation of inhaled ultrafine particles to the brain. *Inhal. Toxicol. 16*:437-445 (2004).

13. Semmler, M., J. Seitz, P. Mayer, et al: Long-term clearance kinetics of inhaled ultrafine insoluble iridium particles from the rat lung, including transient translocation into secondary organs. *Inhal. Toxicol*. *16*:453-459 (2004).

14. Dasenbrock, C., L. Peters, O. Creutzenberg, and U. Heinrich: The carcinogenic potency of carbon particles with and without PAH after repeated intratracheal administration in the rat. *Toxicol. Lett*. *88*:15-21 (1996).

15. Driscoll, K.E., J.M. Carter, B.W. Howard, et al: Pulmonary inflammation, chemokine, and mutagenic responses in rats after subchronic inhalation of carbon black. *Toxicol. Appl. Pharmacol. 136*:327-380 (1996).

16. Shwe, T.T.W., S. Yamamoto, M. Kakeyama, T. Kobayashi, and H. Fujimaki: Effect of intratracheally instillation of ultrafine carbon black on proinflammatory cytokine and chemokine release and mRNA expression in lung and lymph nodes of mice. *Toxicol. Appl. Pharmacol. 209*:51-61 (2005).

17. Nemmar, A., P.H. Hoet, B. Vanquickenborne, et al: Passage of inhaled particles into the blood circulation in humans. *Circulation. 105*:411-414 (2002).

18. Liu, G., P. Mena, P.R.L. Harris, R.K. Rolston, G. Perry G, and M.A. Smith: Nanoparticle iron chelators: A new therapeutic approach in Alzheimer disease and

other neurologic disorders associated with trace metal imbalance. *Neurosci. Lett. 406*:189–193 (2006).

19. U.S. Department of Labor: *Bureau of Labor Statistics (BLS),* Occupational Outlook Handbook, 2016-17 Edition, *Painters, Construction and Maintenance*, on the Internet at https://www.bls.gov/ooh/construction-and-extraction/painters-construction-and-maintenance.htm (visited *June 13, 2017*).

20. IARC (2010). Painting, firefighting, and shiftwork. IARC Monogr Eval Carcinog Risks Hum, 98:1–804.

21. Guha, N., F. Merletti, N.K. Steenland, A. Altieri, V. Cogliano, and K. Straif: Lung Cancer Risk in Painters: A Meta-analysis. *Environ. Health Perspect. 118*:303-312 (2010).

22. U.S. Department of Labor: Bureau of Labor Statistics, Survey of Occupational Injuries and Illnesses, Tables 3, 7 and 8. on the Internet at https://www.bls.gov/news.release/archives/osh2_11102016.pdf (accessed *June 13, 2017*).

23. Kaukiainen, A., R. Martikainen, R. Riala, K. Reijula, and L. Tammilehto: Work tasks, chemical exposure and respiratory health in construction painting. *Am. J. Ind. Med. 51*:1–8 (2008).

24. Kaegi, R., B. Sinnet, S. Zuleeg, et al: Release of silver nanoparticles from outdoor facades. *Environ. Poll. 158*:2900-2905 (2010).

25. Al-Kattan, A., A. Wichser, R. Vonbank, et al: Release of TiO_2 from paints containing pigment-TiO_2 or nano-TiO_2 by weathering. *Environ. Sci.: Processes Impacts 15*:2186-2193 (2013).

26. Künniger, T., A.C. Gerecke, A. Ulrich, et al: Release and environmental impact of silver nanoparticles and conventional organic biocides from coated wooden facades. *Environ. Poll. 184*:464-471 (2014).

27. Fiorentino, B., L. Golanski, A. Guiot, J.-F. Damlencourt, and D. Boutry: Influence of paints formulations on nanoparticles release during their life cycle. *J. Nanopart. Res. 17*:149 (2015).

28. Koponen, I.M., K.A. Jensen, and T. Schneider: Comparison of dust released from sanding conventional and nanoparticle-doped wall and wood coatings. *J. Exp. Sci. Environ. Epidem. 21*:408–418 (2011).

29. Gomez, V., M. Levin, E.T. Saber, et al: Comparison of Dust Release from Epoxy and Paint Nanocomposites and Conventional Products during Sanding and Sawing. Ann. Occup. Hyg. *58*:983-994 (2014).

30. Gohler, D., M. Stinntz, L. Hillemann, and M. Vorbau: Characterization of nanoparticle release from surface coatings by the simulation of a sanding process. *Ann. Occup. Hyg. 54*(6):615-624 (2010).

31. U.S. Department of Agriculture: Wood Handbook. Wood as an Engineering Material. Forest Products Laboratory, General Technical Report FPL-GTR-113. Profest Products Society, Madison, Wisconsin, 1999.

32. Jiang, S., A. Van Dyk, A. Maurice, et al: Design colloidal particle morphology and self-assembly for coating applications. *Chem. Soc. Rev. 46*:3792-3807 (2017).

33. Cooper, M.R., G.H. West, L.G. Burrelli, et al: Inhalation exposure during spray application and subsequent exposure of a wood sealant containing zinc oxide nanoparticles. *J. Occup. Environ. Hyg.*14:510-522 (2017).

34. Fransman, W., C. Bekker, P. Tromp, and W.B. Duis: Potential released of manufactured nano objects during sanding of nano-coated wood surfaces. Ann. Occup. Hyg. 60:875-884 (2016).

35. Federation of European Producers of Abrasives: *Grain standards.* Grains of fused aluminum oxide, silicon carbide and other abrasive materials for coated abrasives Macrogrits P12 to P220 FEPA. 43-1, 2006.

36. Saber, A.T., I.K. Koponen, K.A. Jensen, et al: Inflammatory and genotoxic effects of sanding dust generated from nanoparticle-containing paints and lacquers. *Nanotoxicol. 6(7)*:776-788 (2011).

37. Donaldson, K., V. Stone, A. Clouter, L. Renwick, and W. MacNee: Ultrafine particles. *Occup. Environ. Med. 58*:211-216 (2001).

38. Smulders, S., K. Luyts, G. Bradants, et al: Toxicity of nanoparticles embedded in paints compared with pristine nanoparticles in mice. *Tox. Sci. 141(1)*:132-140 (2014).

39. Sager, T.M., C. Kommineni, and V. Castranova: Pulmonary response to intratracheal instillation of ultrafine versus fine titanium dioxide: Role of surface area. *Part. Fibre Toxicol. 5*:17 (2008).

40. Sager, T.M., and V. Castranova: Surface area of particle administered versus mass in determining the pulmonary toxicity of ultrafine and fine carbon black: comparison to ultrafine titanium dioxide. *Part. Fibre Toxicol*. *6*:15 (2009).

ON THE ROLE OF ATMOSPHERIC CONDITIONS ON PAINT DUST AEROSOL GENERATED FROM MECHANICAL ABRASION OF TiO_2-CONTAINING PAINTS

by

ADAM W. NORED, MARIE-CECILE G. CHALBOT, JACOB S. SHEDD, AND ILIAS G. KAVOURAS

Submitted in preparation for *Earth*

Formatted adapted for dissertation

ABSTRACT

In recent years the introduction and use of new nanomaterials in construction has increased at a rapid rate. Exterior surface paints have been a product that has had these nanomaterials added to them. In this study, the effects of natural weathering and exposure to atmospheric agents was examined to determine the detrimental effects upon outdoor paint that has been created with nanomaterials. Data collected over the course of the yearlong study indicate the nanoparticles of the titanium dioxide were eliminated rapidly. Further testing indicated that various elements of weathering were affecting the physical integrity of the paint. The weathering agents that appear to have the greatest effect on the samples were acid deposition and total precipitation. There was a strong association with carbon monoxide and the effects upon the panels. These results can lead to new plans for assessments involving the synergistic effects of all weathering agents.

Keywords: Meteorology, Air pollutants, Acidity, Titanium dioxide

INTRODUCTION

Engineered nanomaterials (ENMs) have been integrated into construction materials including paints. [1] These nano-enabled products (NEPs) are commercially desirable due to their improved structural integrity, thermal conductivity, fire prevention, and self-cleaning features as compared to conventional products, and as such, they are extensively used in commercially available consumer products. [2–5] Despite these advantages. Most commercially available NEPs are not properly identified as containing nanomaterials. Moreover, knowledge about their health and environmental effects is scarce, particularly throughout the lifecycle of the product. For paint, it includes preparation and application on indoor and outdoor surfaces, environmental weathering and aging, and final removal, typically by mechanical abrasion. Many ENMs, such as carbon nanotubes, silicon dioxide, and copper oxide have been shown to be harmful to humans, with pristine nanoparticles proven to pass from the lungs into the circulatory, lymphatic, and nervous systems. [6–10]

Exposures of painters and other construction workers are most likely to occur at the early and last stages of the paint lifecycle. Sanding dust of walls and wood coated with nano-containing products was dominated by particles in the 100-300 nm size range. [11] TiO_2 and Ag nanoparticles were found in 80% of the collected paint dust particles. [12] The size of TiO_2-containing paint dust and the abundance of nano-sized TiO_2 agglomerates was related to sandpaper grit size. [13] As a result, there is potential for occupational exposures to nanoparticles in paints. This can lead to a rise the possibility of various diseases that involve the lungs, as painters already have consistently higher lung

cancer mortality than other construction workers. [14] Additionally, the probability of a painter to develop COPD is the second highest of all construction workers, following roofers. [15]

Exposure to environmental conditions including weather and chemicals affects the integrity and stability of paint over time leading to deterioration, breaks and release of chemical species. Kaegi et al. [16] determined that leachate from a two-year-old weather exposed façade had significantly less ENMs than a freshly coated façade. Silver ENMs leaching showed that the first two months of exposure resulted in 30% of total ENM loss. [17] Atmospheric pollution can also be detrimental to coatings over time. Acid deposition is known to significantly deteriorate the integrity of outdoor surfaces. [18,19] Titanium dioxide (TiO_2), the most widely used pigment in paints, reacts with acids through photocatalysis leading potentially to the destruction of the coating binders at the outer paint film. [20,21] This may be enhanced by the interaction of anatase nano TiO_2 and UV light. [22] As a result, paint chemicals and ENMs may be released into the environment and enter the human body through a variety of exposure pathways including hand-to-mouth for toddlers, the primary concern for Pb-based pain, and through the food chain (i.e. bioaccumulation). [23-25]

In the present work, we aimed to evaluate the effect of environmental weathering on the release of TiO_2-containing paint dust by mechanical abrasion. The premise behind this study is that environmental weathering may deteriorate the integrity of paint over time affecting both the availability and ease of generation of TiO_2-containing paint dust by mechanical abrasion. Using a previously developed methodological framework, the

current work sought to realistically simulate the generation of TiO_2-containing paint dust by mechanical abrasion on weathered wood panels over a year.

MATERIALS AND METHODS

Weathering

To evaluate the role of environmental weathering on paint dust generated by mechanical abrasion, wood panels painted with TiO_2-containing paint were exposed to weather conditions and air contaminants for regular intervals up to a year. More specifically, both sides of twelve (12) wood panels were prepared, conditioned, and coated as previously described (Nored et al. 2018). The panels were stored in a controlled room (20 °C and 30% RH) for 24 hours before exposure. All panels were placed on the roof of a 6-floor university building with restricted access and at least 10 meters away from major air intake and outlets to prevent unwanted contamination and interference (latitude: 33.502001; longitude: -86.80382 (Datum: WGS84)) from February 1, 2017 to January 31, 2018. Every fifteen days the panels were rotated to directly expose both sides to environmental conditions. A panel was randomly selected every 30 days for mechanical abrasion.

Meteorological conditions and air pollution concentrations measured at the NCore site in Birmingham, Alabama (EPA AIRS ID: 01-073-0023) (latitude: 33.553056; longitude: -86.815000 (Datum: WGS84); Elevation 177 meters above sea level) for 2017 and 2018 period were retrieved from US Environmental Protection Agency's Air Quality System (AQS). Meteorological conditions included hourly temperature (in ^{o}F), percent relative humidity, barometric pressure (in mbar), total precipitation (in inches of water),

resultant wind speed (in knots) and solar radiation (in Langley per minute) were collected. Criteria gaseous pollutants included hourly CO (in ppm), O_3 (in ppm), NOx (in ppb), SO_2 (in ppv). Daily PM_{10} and $PM_{2.5}$ mass (in $\mu g\ m^{-3}$) and PM2.5 speciation data were obtained in a once every 3 days frequency. More specific, total sulfate, nitrate, ammonium bisulfate, and ammonium nitrate concentrations were obtained.

PAINT DUST GENERATION AND CHARACTERIZATION

The Coatings Aerosol Resuspension System (CARES) was used to generate TiO_2 containing paint dust using an orbital sander and 120 grit size sandpaper in a polyvinylchloride glove box chamber (115 cm x 60 cm x 60cm) (Lancs Industries, Kirkland, WA) (Nored et al. 2018). A wide particle spectrometer (WPS) (Model 1000XP, MSP Corp., Shoreview, MN) and a condensation particle counter (CPC) (Model 3771, TSI Inc., Shoreview, MN) were used to measure particle number concentration and size distribution. Paint dust samples were collected on 13-mm cellulose filters and 47-mm Teflon filters (Pall Corp., Port Washington, NY) at 1.0 and 5.0 L min^{-1} flow rate, respectively, for chemical and imaging analysis, respectively. Chemical analysis was done by attenuated total reflectance Fourier-transform infrared spectrometer (ATR-FTIR; ALPHA II Platinum ATR, Bruker corp., Billerica, MA) with a single reflection diamond ATR (range: 400-4000 cm^{-1}, with a resolution of 2 cm^{-1}). Morphological analysis was performed by scanning electron microscope (SEM; 650 FEG, Eindhoven, the Netherlands). The SEM was used in low pressure setting at 0.53 torr, working distance of 10mm. and accelerating voltage at 10 kV. Samples were examined at 5000x and 10000x

magnification. Elemental composition was determined using the integrated energy-dispersive X-ray (EDX) at 5000x magnification.

DATA ANALYSIS

The count median diameter (CMD), geometric standard deviation (GSD), and PM_{10}, $PM_{2.5,}$ and $PM_{1.0}$ mass concentration of paint dust were computed using the WPS data as previously described (Nored et al. 2018). Daily descriptive statistics or meteorological and air pollution variables were computed from hourly measurements. Subsequently, daily estimates were further aggregated to compute the cumulative exposure conditions for each wood panel over the 48-week period. Aerosol acidity (in mol m^{-3}) was computed as the sum of the molar concentrations of free sulfate (difference of total and neutralized (and ammonium bisulfate) sulfate), and free nitrate (difference of total and neutralized (and ammonium nitrate) nitrate). The sum of gaseous SO_2 and NO_x molar concentrations (in mol m^{-3}) was defined as the gas acidity. Ordinary least squares regression analyses of CMD, GSD, $PM_{2.5}$ and $PM_{1.0}$ mass, and source contributions were used to determine the monthly trends. Multivariate least squares linear regression analysis was used to estimate the synergistic effect of weathering conditions on paint dust levels. The following weather conditions were included in the analysis: dew point (computed from ambient temperature, percent relative humidity and barometric pressure), molar CO and O_3 concentrations, precipitation, wind speed and aerosol and gas acidity, allowing for *df=4* (degrees of freedom of the model). The percent relative effect of each variable was calculated as the product of the regression coefficient and cumulative exposure for each variable to the total effect of all variables. The intercept is interpreted to be the effect

associated with other weathering variables not included in this study such as highly reactive radicals. All analyses were done using SPSS (Version 23; IBM Analytics, Armonk, NY) and Origin Pro (Version 9.1; OriginLab, Northampton, MA).

RESULTS AND DISCUSSION

Paint Dust Concentrations and Trends

Table 1 presents the mean (± 3 × standard error) and monthly trend of the CMD, GSD, and reconstructed PM_{10}, $PM_{2.5}$ and $PM_{1.0}$ mass concentrations. The CMD of paint dust varied from 39 ± 10 nm to 98 ± 29 nm with a monthly increase of 2.2 ± 1.2 nm mo^{-1}. The GSDs of paint dust particles decreased from 3.9 ± 0.7 to 2.3 ± 0.1, at a rate of 0.12 ± 0.02 nm mo^{-1}, suggesting a narrow size range of paint dust particles after weathering. The CMD and GSD of paint dust generated after 1 month of environmental weathering were somewhat different than those computed for paint dust generated from freshly painted wood panels using the same protocol (CMD of 39.4 ± 2.7 nm; GSD of 2.2 ± 0.1) albeit similar levels of particle mass (PM_{10}, $PM_{2.5}$**,** and PM_1) levels were generated. It may be suggestive of weathering processes affecting the physical integrity of paints and therefore the number and size of generated paint dust but with no significant changes in the availability of paint. The PM_{10}, $PM_{2.5}$**,** and PM_1 paint dust concentrations varied month-by-month; however, an overall decline was observed for all three fractions, from -123 ± 35 μg m^{-3} mo^{-1} for PM_{10}, to -5 ± 3 μg m^{-3} mo^{-1} for $PM_{2.5}$ and -1 ± 0.8 μg m^{-3} mo^{-1} for PM_1. This trend indicated that weathering may reduce the quantity of paint available for mechanical abrasion through physical and chemical deterioration and break-up.

Table 1. Monthly paint dust CMD, GSD and mass concentrations and trend (mean ± 3×standard error)

Duration (mo)	CMD (nm)	GSD	Particle mass ($\mu g/m^3$)		
			PM_{10}	$PM_{2.5}$	$PM_{1.0}$
1	60 ± 22	3.4 ± 0.5	1,250 ± 715	71 ± 43	18 ± 11
2	52 ± 12	3.9 ± 0.7	1,573 ± 833	84 ± 39	22 ± 10
3	51 ± 14	2.9 ± 0.5	764 ± 471	38 ± 20	10 ± 5
4	77 ± 28	2.9 ± 0.5	1,443 ± 1023	92 ± 68	25 ± 19
5	68 ± 18	2.8 ± 0.5	1,887 ± 2325	130 ± 143	37 ± 8
6	62 ± 8	2.8 ± 0.2	832 ± 353	79 ± 36	24 ± 11
7	39 ± 10	2.5 ± 0.1	247 ± 166	25 ± 16	9 ± 6
8	50 ± 12	2.7 ± 0.2	315 ± 154	26 ± 17	8 ± 5
9	61 ± 12	2.5 ± 0.1	373 ± 416	38 ± 32	12 ± 8
10	69 ± 10	2.3 ± 0.1	315 ± 225	39 ± 22	13 ± 7
11	98 ± 29	2.4 ± 0.2	577 ± 380	64 ± 27	22 ± 7
12	82 ± 9	2.3 ± 0.1	118 ± 78	13 ± 9	4 ± 3
Trend	2.2 ± 1.2 ($nm\ mo^{-1}$)	-0.12 ± 0.02 (mo^{-1})	-123 ± 35 ($\mu g\ m^{-3}\ mo^{-1}$)	-5 ± 3 ($\mu g\ m^{-3}\ mo^{-1}$)	-1 ± 0.8 ($\mu g\ m^{-3}\ mo^{-1}$)

Chemical and Morphological Analysis

The ATR-FTIR absorbance spectra of paint dust at 0, 3, and 12 months are depicted in Fig. 1. All paint dust samples retained the absorption bands in the 1500 – 3500 cm^{-1} from wood cellulosic signatures and paint organic polymers [13,26]. However, there was a decline in the absorption bands in the 1240 - 750 cm^{-1}, attributed to stretching of =C-H and C-O groups and bending vibration of the aromatic C-H groups. Olefinic, aromatic, and hydroxyl functional groups may be more susceptible to reactions by atmospheric oxidants leading to re-arrangement and break-up of the aliphatic chain in organic polymers and/or hydrogen bonds between polymers [27,28]. The abundance of broad bands in the 400 – 650 cm^{-1} region previously assigned to TiO_2 was observed to substantially decline following 3 months of environmental weathering, indicating the rapid elimination of TiO_2 materials from painted surfaces due to weathering.

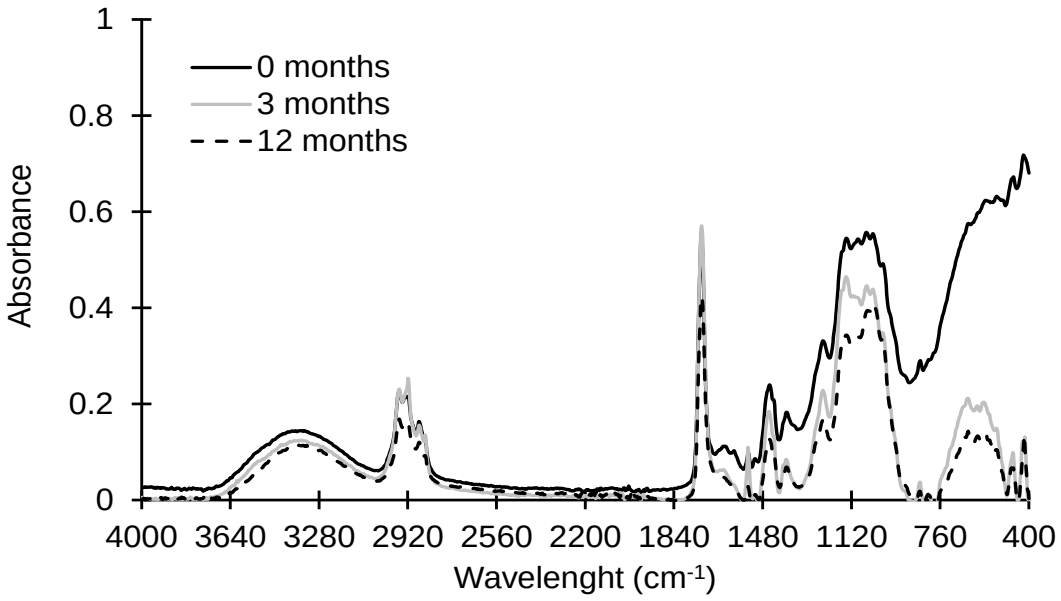

Figure 1. ATR-FTIR spectra of paint dust generated by sanding using P120 sandpaper after 0-, 3- and 12-months of environmental weathering

Fig. 2 depicts the SEM backscattering images of paint dust at months 0, 3, and 12. Released paint dust particles contained TiO_2 nanomaterials in various shapes (spherical, amorphous) in the nano-size and submicron size range at 0 months. Both the size and concentration of TiO_2 paint dust agglomerates declined following weathering indicating that most of the TiO_2 may be inadvertently released into the environment, however, the remaining TiO_2 may be released in the nano size range by mechanical abrasion.

Figure 2**.** Backscattering SEM image of paint dust generated by sanding using P120 sandpaper after 0 (A), 3 (B) and 12 (C) months environmental weathering.

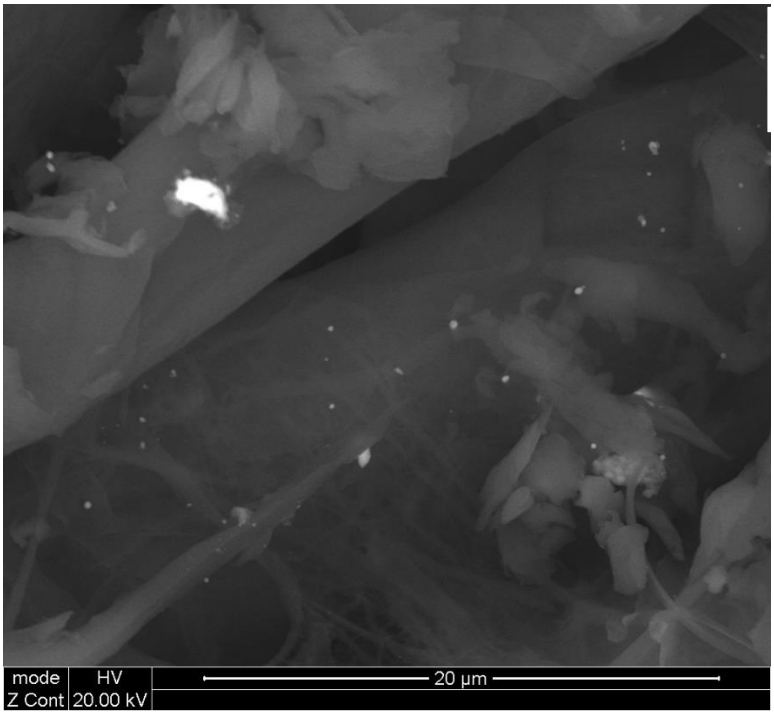

A

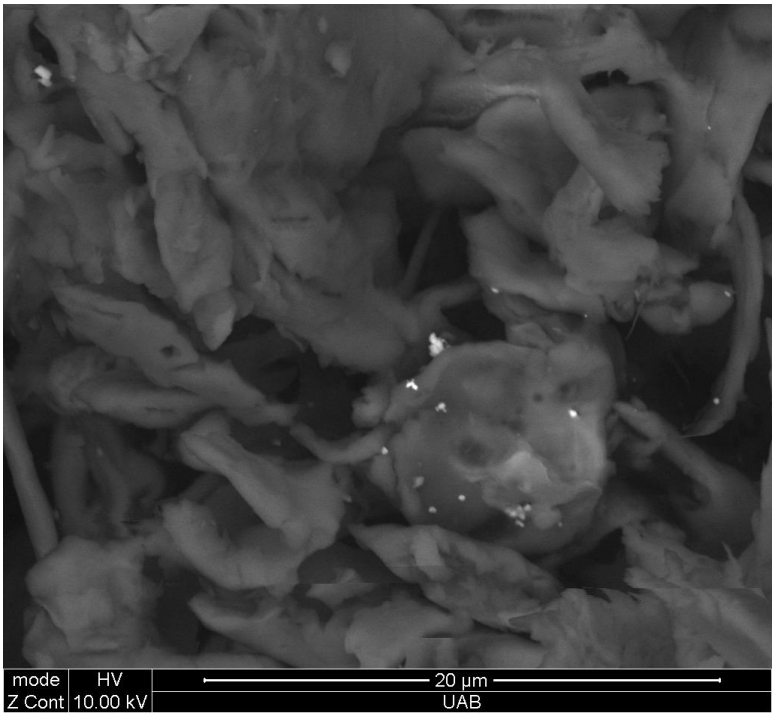

B

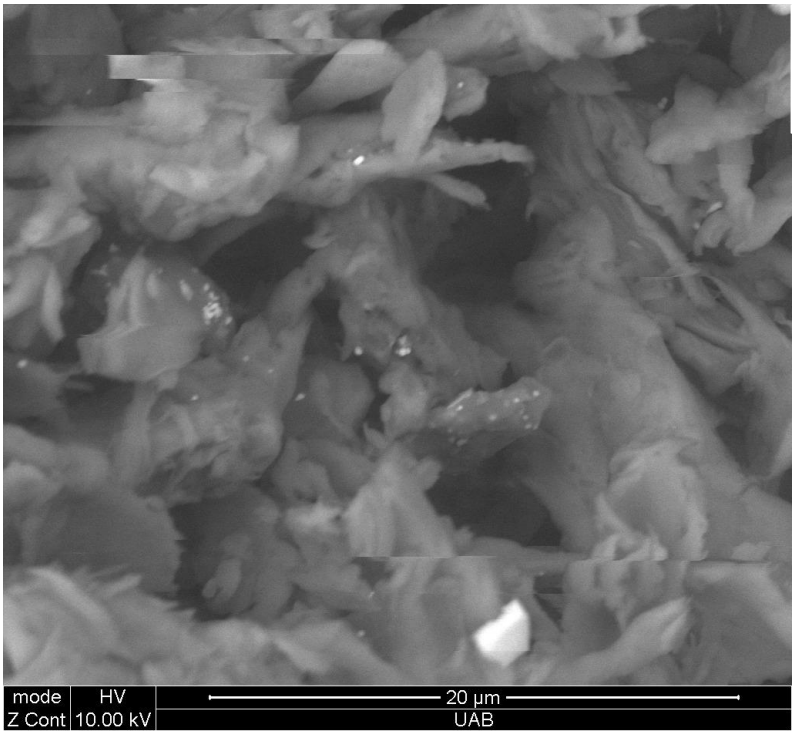

C

Weathering

Figs. 3-5 show the daily variation of meteorological, gas and particulate pollutants with the study period. The mean daily temperature and relative humidity were 64.9 ^{o}F and 66%, respectively. There was a total of 123 rain events for a total of 2.65 inches of water. The winds were blowing from variable direction, mostly across the southwest-northeast axis up to 8 knots, on average. The mean daily CO, O_3, NO_x, and SO_2 concentrations were 360 ppb, 23 ppb, 14 ppb, and 9 ppb, respectively. The mean daily ambient PM_{10} and $PM_{2.5}$ mass concentrations were 45.8 and 8.8 µg m^{-3}, indicating that a large fraction of ambient PM_{10} was composed of coarse particles. Total sulfate and nitrate concentrations (2.7 µg m^{-3} and 0.9 µg m^{-3}) were substantially higher than those computed from neutralized ammonium bisulfate (2.09 µg m^{-3}) and ammonium nitrate (0.6 µg m^{-3}), suggesting acidic aerosol conditions that favor deposition of sulfuric and nitric acid to

surfaces. The variation of meteorological and air pollution conditions was typical of an urban environment.

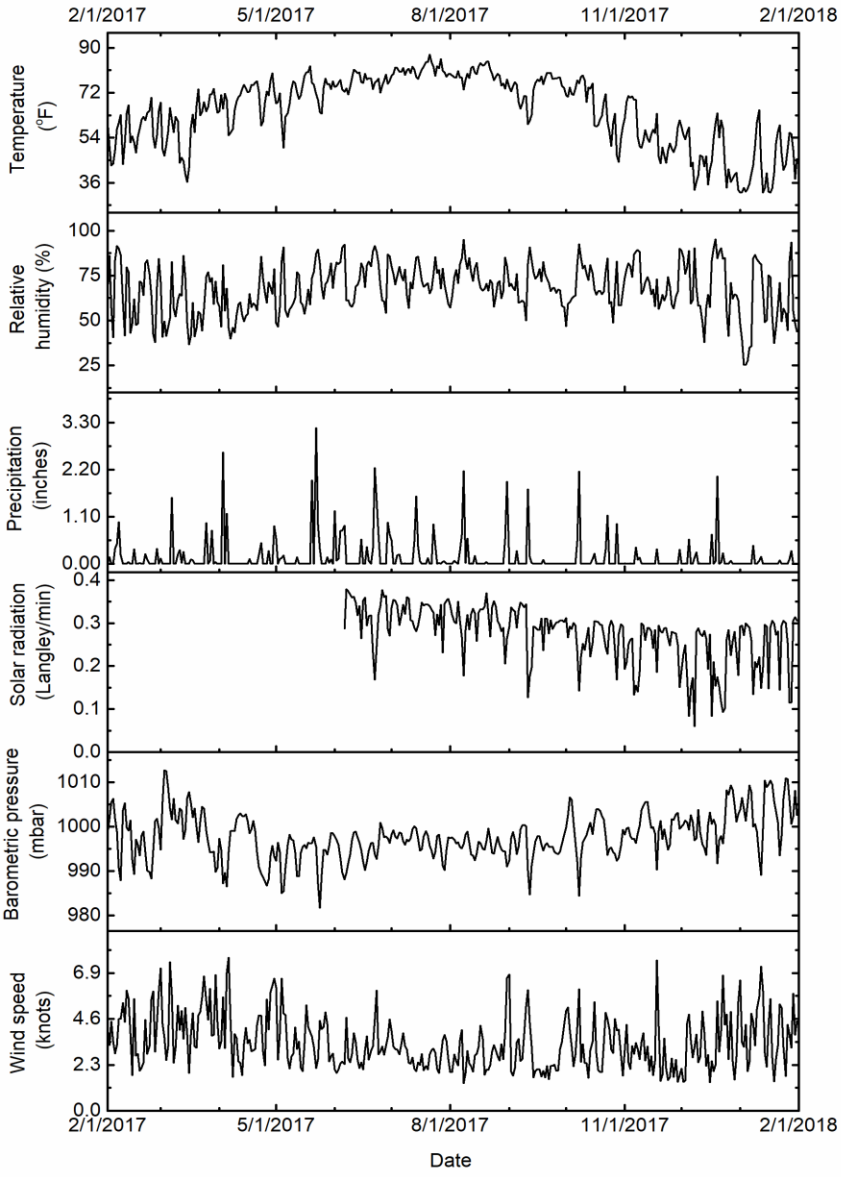

Figure 3. Daily temperature (a, in ^{o}F), relative humidity (b, %), precipitation (c, inches of H_2O), solar radiation (d, Langleys/min) and resultant wind speed (e, knots)

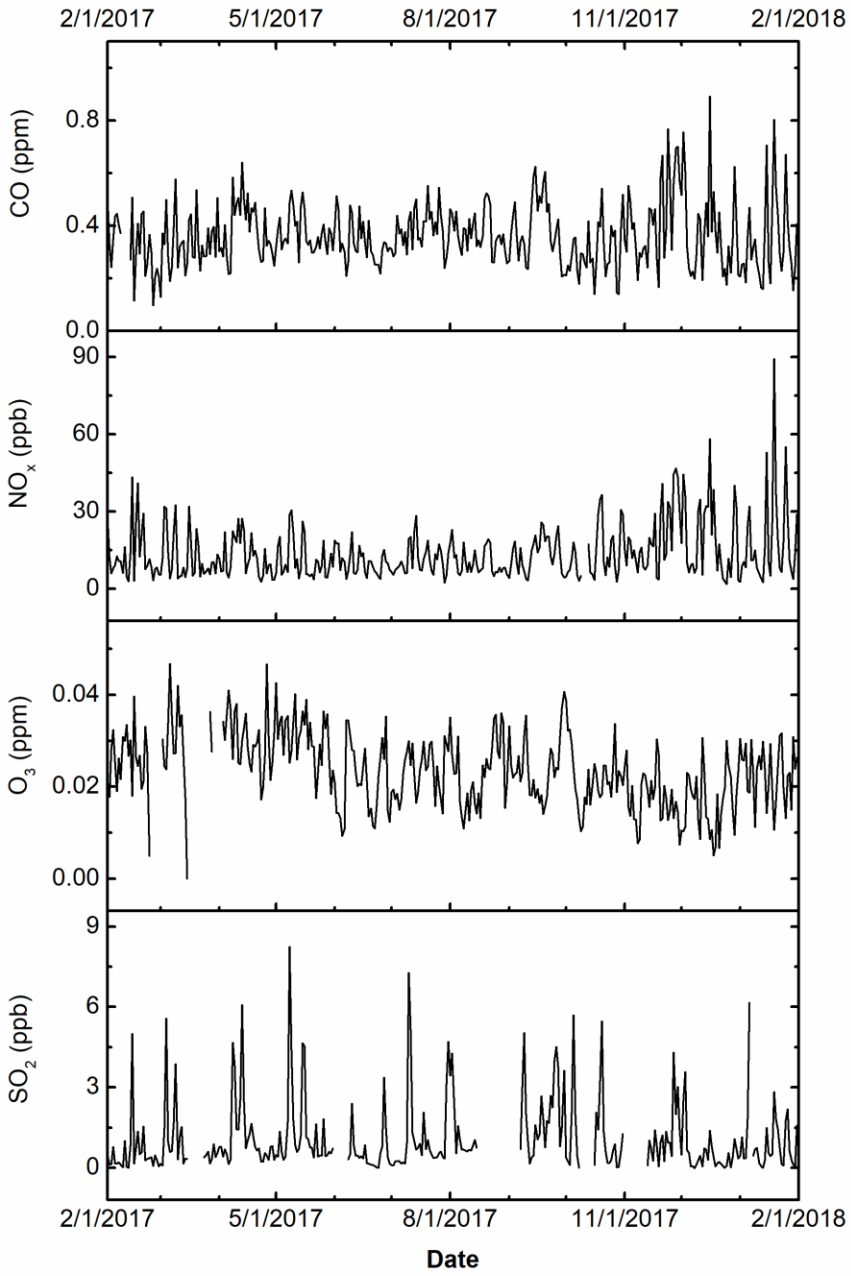

Figure 4. Daily carbon monoxide (a, in ppm), nitrogen oxides (b, ppb), ozone (c, ppm) and sulfur dioxide (d, in ppb).

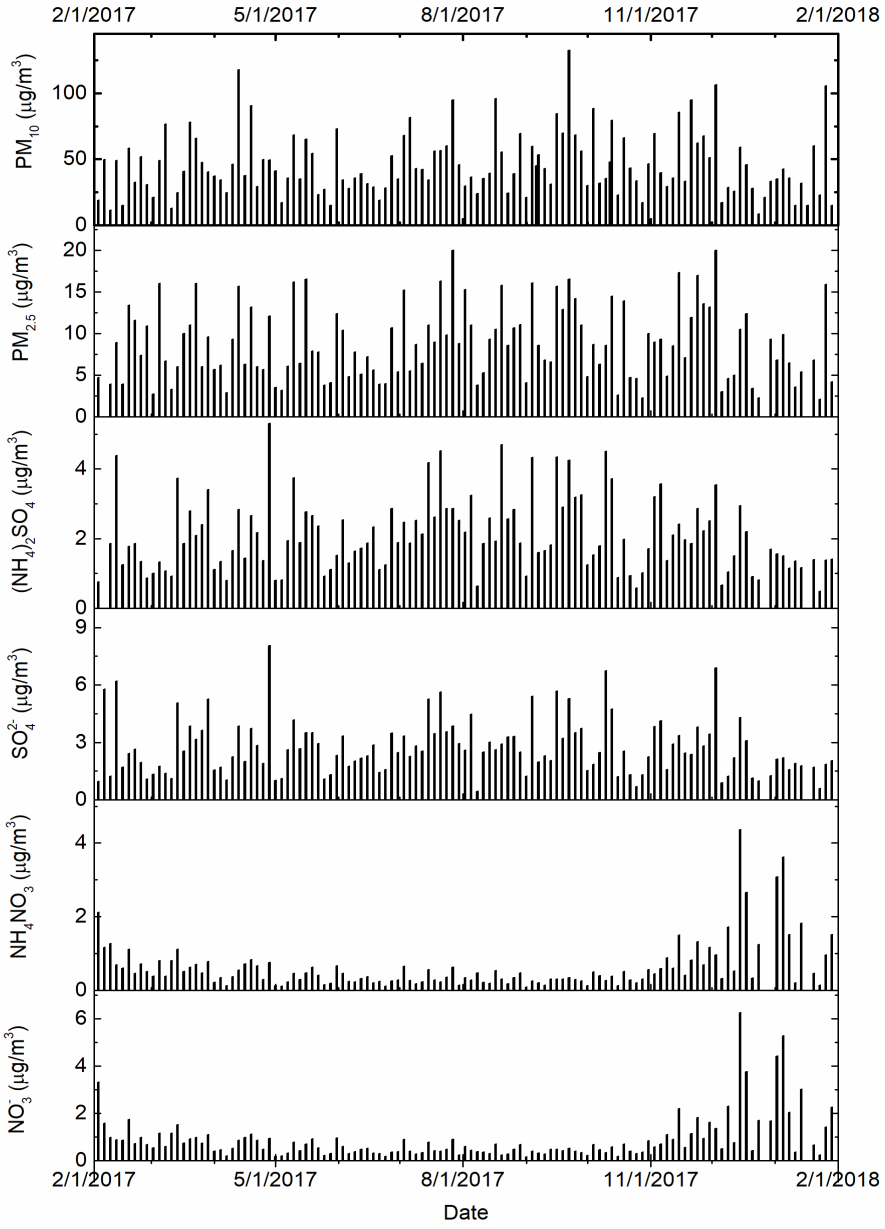

Figure 5. Daily PM_{10} (a), $PM_{2.5}$ (b), ammonium bisulfate (c), ammonium nitrate (d), total sulfate (e) and total nitrate (f) concentration (in $\mu g/m^3$).

Fig. 6 shows the percent relative effect of weathering factors of paint dust CMD, GSD, $PM_{2.5}$ and PM_1 mass concentrations. The overall effect of meteorological conditions (dew

point, rain, and wind) was positive, i.e. more paint dust being generated by abrasion, probably due to physical decomposition of paint and wood. The negative relative effect of CO and aerosol acidity for CMD and GSD indicated that smaller particles may be generated and therefore, the resultant $PM_{2.5}$ and PM_1 paint dust mass would decline, as computed by the regression analysis. On the other hand, exposure to strong gas oxidants such as O_3, NO_x and SO_2 may result in the generation of larger particle that was associated with an increase of paint dust mass.

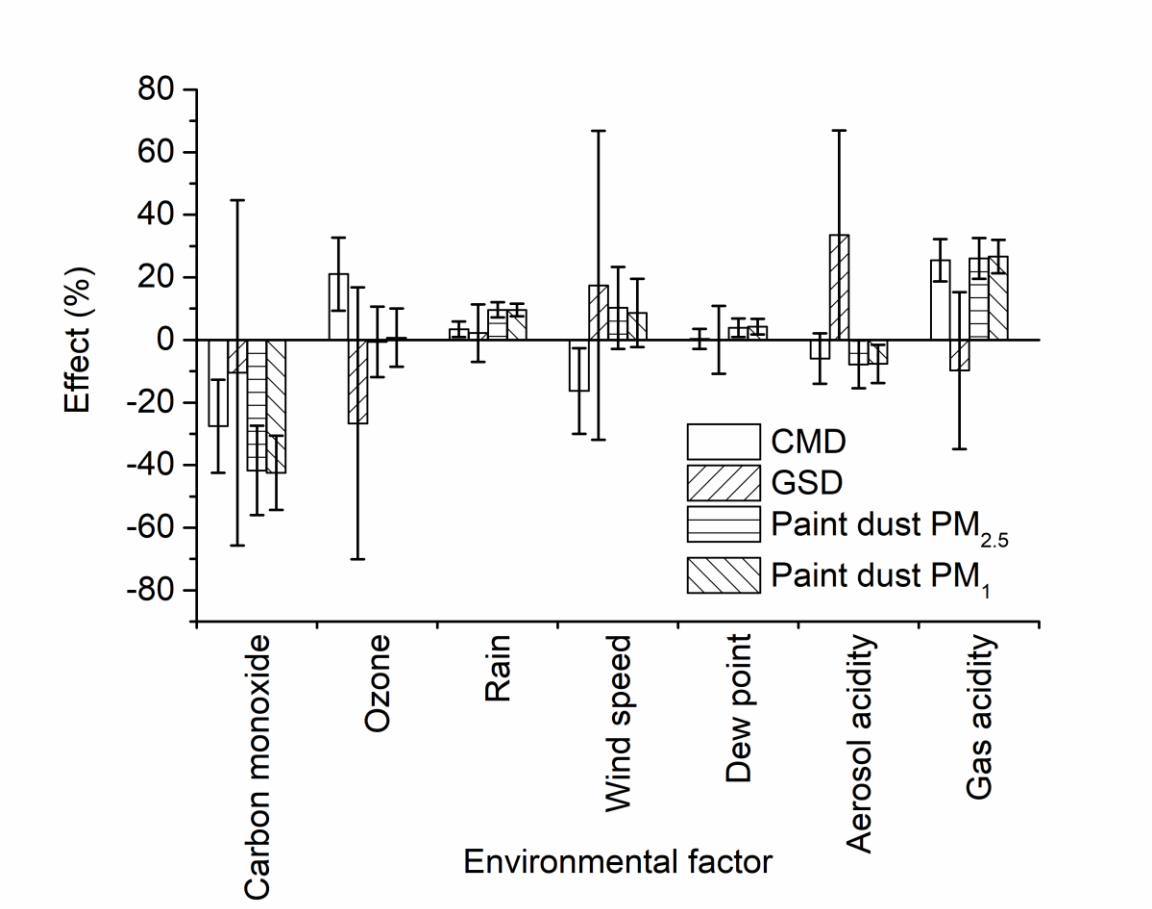

Figure 6. Effect (%) of environmental weathering conditions on paint dust $PM_{2.5}$, PM_1, CMD and GS

Degradation of painted surfaces exposed to weathering occur at the surface of the paint, inside the paint layer and at the interface between the film and the substrate. Weathering conditions degrade painted surfaces through chain-scission and cross-linking reactions in the paint layer, deteriorating adhesion and the mechanical compatibility with the substrate. Previous studies clearly demonstrated the capacity of oxidative agents (e.g. acid rain, ozone and radicals) to inadvertently cause significant damage to painted surfaces [29]. However, there is no evidence of chemical interactions of paint formulations, TiO_2 materials and CO [30]. In an urban environment, CO is released predominantly from automobiles. Traffic exhaust is also the primary source of volatile organic compounds that can readily react in the atmosphere and form hydroxyperoxy radicals. Paints may undergo oxidation and isomerization from a non-conjugated to a conjugated isomer, and form hydroperoxides at allylic and vinylic carbons. This was in agreement with changes in the FTIR spectra of paint dust. These hydroperoxides may form dimers and polymers to an insoluble and infusible film. These reactions may occur throughout the life of the paint but at decreasing rates.

Water also accelerates deterioration by stimulating physical processes and volatile and water-soluble decomposition byproducts. In conjunction with high ambient temperature, that is typical in the southeast US, degradation reactions may accelerate depending on the reactions' activation energy. These processes may be further facilitated by TiO_2 particles. Anatase titanium dioxide participates chemically in the deterioration reaction by acting as catalyst in the oxidation of film by atmospheric oxygen. [2]

CONCLUSIONS

All painted surfaces are sensitive to environmental weathering. They undergo photodegradation, leaching, hydrolysis, swelling, discoloration, and degradation. This study showed that most of TiO_2 and paint polymers may have been depleted from weathered painted surfaces; however, paint dusts generated by abrasion contained TiO_2 agglomerates in the nano size range. Weathering agents including meteorological conditions and air pollutants act at different levels, rates, independently or synergistically in various combinations and in different sequences resulting in highly variable outcomes**,** which declined over time. Gas and aerosol acidity and rain appeared to exert a strong influence on paint deterioration. The strong association with carbon monoxide may be due to strong correlation of CO with co-emitted, highly-reactive volatile organic compounds from vehicles. This study demonstrated the need to assess the synergistic effects of environmental weathering on painted surfaces because of its potential for the release of appreciable quantities of TiO_2-containing paint dust in the environment and in workers.

REFERENCES

[1] Buzea C, Pacheco II, Robbie K. Nanomaterials and nanoparticles: Sources and toxicity. Biointerphases 2007;2:MR17–71.

[2] Carp O, Huisman CL, Reller A. Photoinduced reactivity of titanium dioxide. Prog Solid State Chem 2004;32:33–177. doi:10.1016/j.progsolidstchem.2004.08.001.

[3] Gladis F, Eggert A, Karsten U, Schumann R. Prevention of biofilm growth on man-made surfaces: Evaluation of antialgal activity of two biocides and photocatalytic nanoparticles. Biofouling 2010;26:89–101. doi:10.1080/08927010903278184.

[4] Dallas P, Sharma VK, Zboril R. Silver polymeric nanocomposites as advanced antimicrobial agents: Classification, synthetic paths, applications, and perspectives. Adv Colloid Interface Sci 2011;166:119–35. doi:10.1016/j.cis.2011.05.008.

[5] Hanus MJ, Harris AT. Nanotechnology innovations for the construction industry. Prog Mater Sci 2013;58:1056–102. doi:10.1016/j.pmatsci.2013.04.001.

[6] Lee J, Mahendra S, Alvarez PJJ. Nanomaterials in the construction industry: A review of their applications and environmental health and safety considerations. ACS Nano 2010;4. doi:10.1021/nn100866w.

[7] Hoet PH, Brüske-Hohlfeld I, Salata O V. Nanoparticles – known and unknown health risks. J Nanobiotechnology 2004;2:12. doi:10.1186/1477-3155-2-12.

[8] Oberdörster G, Oberdörster E, Oberdörster J. Nanotoxicology: An emerging discipline evolving from studies of ultrafine particles. Environ Health Perspect 2005;113:823–39. doi:10.1289/ehp.7339.

[9] Liu J, Wong HL, Moselhy J, Bowen B, Wu XY, Johnston MR. Targeting colloidal particulates to thoracic lymph nodes. Lung Cancer 2006;51:377–86. doi:10.1016/j.lungcan.2005.11.006.

[10] Oberdörster G, Sharp Z, Atudorei V, Elder A, Gelein R, Kreyling W, et al. Translocation of inhaled ultrafine particles to the brain. Inhal. Toxicol., vol. 16, 2004, p. 437–45. doi:10.1080/08958370490439597.

[11] Koponen IK, Jensen KA, Schneider T. Comparison of dust released from sanding conventional and nanoparticle-doped wall and wood coatings. J Expo Sci Environ Epidemiol 2011;21:408–18. doi:10.1038/jes.2010.32.

[12] Gomez V, Levin M, Saber AT, Irusta S, Maso MD, Hanoi R, et al. Comparison of dust release from epoxy and paint nanocomposites and conventional products during sanding and sawing. Ann Occup Hyg 2014;58:983–94. doi:10.1093/annhyg/meu046.

[13] Nored AW, Chalbot M-CG, Kavouras IG. Characterization of paint dust aerosol generated from mechanical abrasion of TiO<inf>2</inf>-containing paints. J Occup Environ Hyg 2018;15. doi:10.1080/15459624.2018.1484126.

[14] Guha N, Merletti F, Steenland NK, Altieri A, Cogliano V, Straif K. Lung cancer risk in painters: A meta-analysis. Environ Health Perspect 2010;118:303–12. doi:10.1289/ehp.0901402.

[15] Ringen K, Dement J, Welch L, Dong XS, Bingham E, Quinn PS. Risks of a lifetime in construction. Part II: Chronic occupational diseases. Am J Ind Med 2014;57:1235–45.

[16] Kaegi R, Ulrich A, Sinnet B, Vonbank R, Wichser A, Zuleeg S, et al. Synthetic TiO2 nanoparticle emission from exterior facades into the aquatic environment. Environ Pollut 2008;156:233–9. doi:https://doi.org/10.1016/j.envpol.2008.08.004.

[17] Kaegi R, Sinnet B, Zuleeg S, Hagendorfer H, Mueller E, Vonbank R, et al. Release of silver nanoparticles from outdoor facades. Environ Pollut 2010;158:2900–5. doi:10.1016/j.envpol.2010.06.009.

[18] Wang X, Kumagai S, Kobayashi K, Yoshimura N. Investigation on surface contamination performances of outdoor polymer insulator aged by artificial acid rain. IEEJ Trans Fundam Mater 1998;118:502–8.

[19] Larssen T, Seip HM, Semb A, Mulder J, Muniz IP, Vogt RD, et al. Acid deposition and its effects in China: an overview. Environ Sci Policy 1999;2:9–24. doi:https://doi.org/10.1016/S1462-9011(98)00043-4.

[20] Giraldo AL, Peñuela GA, Torres-Palma RA, Pino NJ, Palominos RA, Mansilla HD. Degradation of the antibiotic oxolinic acid by photocatalysis with TiO2 in suspension. Water Res 2010;44:5158–67. doi:https://doi.org/10.1016/j.watres.2010.05.011.

[21] Bahnemann DW, Kholuiskaya SN, Dillert R, Kulak AI, Kokorin AI. Photodestruction of dichloroacetic acid catalyzed by nano-sized TiO2 particles. Appl Catal B Environ 2002;36:161–9. doi:https://doi.org/10.1016/S0926-3373(01)00301-0.

[22] Marolt T, Škapin AS, Bernard J, Živec P, Gaberšček M. Photocatalytic activity of anatase-containing facade coatings. Surf Coatings Technol 2011;206:1355–61. doi:https://doi.org/10.1016/j.surfcoat.2011.08.053.

[23] Lin GZ, Peng RF, Chen Q, Wu ZG, Du L. Lead in housing paints: An exposure source still not taken seriously for children lead poisoning in China. Environ Res 2009;109:1–5. doi:10.1016/j.envres.2008.09.003.

[24] Lucas JP, Le Bot B, Glorennec P, Etchevers A, Bretin P, Douay F, et al. Lead contamination in French children's homes and environment. Environ Res

2012;116:58–65. doi:10.1016/j.envres.2012.04.005.

[25] Rizwan M, Ali S, Qayyum MF, Ok YS, Adrees M, Ibrahim M, et al. Effect of metal and metal oxide nanoparticles on growth and physiology of globally important food crops: A critical review. J Hazard Mater 2017;322:2–16. doi:10.1016/j.jhazmat.2016.05.061.

[26] Vahur S, Teearu A, Leito I. ATR-FT-IR spectroscopy in the region of 550–230 cm−1 for identification of inorganic pigments. Spectrochim Acta Part A Mol Biomol Spectrosc 2010;75:1061–72. doi:10.1016/J.SAA.2009.12.056.

[27] Stephens ER. Chemistry of atmospheric oxidants. J Air Pollut Control Assoc 1969;19:181–5.

[28] Minakata D, Li K, Westerhoff P, Crittenden J. Development of a group contribution method to predict aqueous phase hydroxyl radical (HO•) reaction rate constants. Environ Sci Technol 2009;43:6220–7.

[29] Lipfert FW, Dupuis LR, Malone RG, Schaedler J. Case study of materials damage due to air pollution and acid rain in New Haven, CT. Brookhaven National Lab., Upton, NY (USA); 1985.

[30] Salthammer T, Fuhrmann F. Photocatalytic surface reactions on indoor wall paint. Environ Sci Technol 2007;41:6573–8. doi:10.1021/es070057m.

THE EFFECT OF PARTICLE SIZE, MEMBRANE TYPE, AND FACE VELOCITY ON TIO2-CONTAINING PAINT DUST FILTRATION

by

ADAM W. NORED, MARIE-CECILE G. CHALBOT, JIN Y. SHIN AND ILIAS G. KAVOURAS

Journal of the International Society for Respiratory Protection 38(1), pp.16-25

Format adapted and errata corrected for dissertation

ABSTRACT

The U.S. Centers of Diseases Control suggests the use of filtering facepiece respirators (FFRs) for painters and related construction occupations. Engineered titanium dioxide (TiO_2) nanoparticles, shown to be more tumorigenic than bulk TiO_2, are prevalent in paint formulations. Specific occupational protection protocols are developed to manage tasks associated with TiO_2-containing paints and dust. In this study, the efficacy of different types of filtration membranes, namely, packed polypropylene (used in N95 FFRs), cellulose acetate, polycarbonate and polytetrafluoroethylene to remove paint dust containing TiO_2 nanoparticles was examined at various conditions. The particle mass size distribution of paint dust was measured using real-time 10-stage Quartz Crystal Microbalance (QCM) cascade impactor. Particles above 300 nm were more efficiently removed by cellulose acetate and polytetrafluoroethylene membranes. The filtration efficiency dropped rapidly for smaller particles in the 100-300 nm range. The results showed that the filtration efficiency of packed polypropylene membrane increased as particle size decreased with the highest computed for particles below 100 nm. This may be due diffusion by Brownian motion and electrostatic attraction. The low collection efficiency of cellulose acetate for the most penetrating and harmful particles below 100 nm was improved by increasing the face velocity. These results can be used by manufacturers to select materials for their respirators. The results can also facilitate future studies on the design and optimization of respirators using polypropylene or cellulose acetate membranes to remove the most potent TiO_2-containing ultrafine paint dust particles.

Keywords: Engineered TiO_2 nanoparticles, paint dust, ultrafine particles, N95 membrane, cellulose acetate

INTRODUCTION

Since 1973, occupational and environmental protections agencies such CDC, Occupational Safety and Health Administration (OSHA) and US Environmental Protection Agency (EPA) have been dealing with Pb-based paints consequences. Yet, an equally harmful and detrimental public health emergency may be brewing due to nanoparticles (NPs) containing paints (Muller *et al* 2018). TiO_2 is the most used (ca. 70% of the total pigments) white pigment in paints because of their high stability, anticorrosive and antibacterial properties. TiO_2 exists in different particle size fractions as fine particles (FPs) (diameter 0.1-2.5 μm) and nanoparticles (NPs) (diameter < 0.1 μm or 100 nm) (Ortlieb *et al* 2010). TiO_2 NPs embedded into paint may be less harmful because of agglomerates formation; however, they are released upon degradation during weathering and sanding. The major exposure route of TiO_2 NP is inhalation in occupational settings. Sanding dust coated with nanoparticle containing paint was dominated by nano size particles (<300 nm) containing up to 80% TiO_2 and other NPs (Koponen *et al* 2015; Nored *et al* 2018).

Upon entry into the human body, TiO_2 NPs are absorbed and translocated across the air-blood barrier, distributed to organs and tissues by systemic circulation and interact with plasma–proteins, coagulation factors, platelets, and blood cells (Geiser *et al* 2010; Lee *et al* 2011; Eydner *et al* 2012). In vivo studies demonstrated the carcinogenic potential of TiO_2 NPs, with TiO_2 NPs being more tumorigenic than TiO_2 FPs on an equal mass dose basis (Trochimowicz *et al* 1988; Heinrich *et al* 1995). Owing on their relative short time in use, initial epidemiological studies did not detect an association between occupational exposures to TiO_2 particles and an increased lung cancer risk (Fryzek *et al* 2003).

Moreover, the association of TiO_2 particle size, the most important determinant of TiO_2 NPs carcinogenicity, with lung cancer risk is not well studied. It is estimated that lifetime occupational exposures of TiO_2 NPs from 70 $\mu g/m^3$ to 700 $\mu g/m^3$ are associated with 0.1% excess risk of lung cancer (Dankovic *et al* 2007). Exposure and dose- response analysis across the lifecycle of products is seriously lacking for both occupational and environmental scenarios particularly in relation to particle size and processes generating high TiO_2 NPs concentrations. It is, therefore, appropriate to control and mitigate TiO_2 NPs exposures to reduce the burden on occupational health and safety, particularly for painters who already have high prevalence lung diseases, such as cancer (Lim et al., 2012), and chronic obstructive pulmonary disease (COPD) (Wang et al., 2016). Paint dust emissions is the ninth leading cause of disease in the coatings industry (Ringen et al., 2014).

The US OSHA recommended an exposure limit for TiO_2 NPs at 0.3 mg/m^3 (NIOSH 2011). TiO_2 NPs are also classified by the International Agency for Research of Cancer (IARC) as a Group 2B (possibly carcinogenic to humans) agent suggesting the products containing TiO_2 NPs should be managed cautiously (Baan 2007). Yet, more than 80% of workers and most consumers are not aware about the presence of NPs in paints (West *et al* 2016). Personal protective equipment such as N95 FFRs (i.e., remove at least 95% of particles with diameter of 0.3 μm (or 300 nm)) have demonstrated a decline in filtration of particles in 20-100 nm size range (may exceed 5%) with the most penetrating particle size of approximately 50 nanometers (Erniger *et al* 2008). *P*re-charged fiber filters have the poorest protection from particles between 35-70 nanometers (Balazy *et al* 2005).

The goal of the study was to assess the efficiency of filtration membranes used for respiratory protection including polypropylene in N95 FFRs (i.e., designed to remove at

least 95% of all airborne particles to remove ultrafine paint dust particles containing engineered TiO_2 nanoparticles. In addition, the effects of particle size and face velocity was examined. Large porosity polycarbonate membrane was used to validate the role of porosity of particle filtration. Realistic TiO_2-containing paint dust was generated using a previously developed experimental apparatus (Nored *et al* 2018). Organic-based paint agglomerates included titanium dioxide NPs predominantly for particles with sizes < 100 nm. This was consistent with previous studies showing the accumulation of engineered NPs in ultrafine paint dust (Koponen *et al* 2011).

MATERIALS AND METHODS

Materials

A commercially available latex paint and primer formulation for indoor surfaces was used to coat wood panels. It was composed of water (49.6% w/w), non-volatile species (49.4% w/w), organic volatiles (0.9% w/w) and 2-amino-2-methyl-1-propanol (0.2% w/w) (CAS #: 124-68-5), TiO_2 (3.2% w/w) (CAS #: 13463-67-7), crystalline silica (0.22% w/w) (CAS #: 14808-60-7) and cristobalite (0.11% w/w) (CAS #: 14464-46-1). For abrasion, a BDERO600 2.4 Amp 5 inches (12.7 cm) orbital sander in its complete configuration (including the fitted filter) (Black & Decker, Towson, MD) fitted with Shopsmith® 5 inches (12.7 cm) aluminum oxide abrasive film discs with 120 grit (Shopsmith, Dayton, OH). The four membranes chosen were cellulose acetate (0.2µm pore size, 47-mm, Pall, MI), polytetrafluoroethylene (PTFE) (2.0µm, pore size, 47-mm, SKC Inc, PA), polycarbonate (Nuclepore®) (8 µm, pore size, 47-mm, Corning, NY) and polypropylene (N95, 3M 8210, St. Paul, MN).

Paint Dust Generation and Measurement

The Coatings Aerosol Resuspension System (CARES) was used to generate TiO_2 containing paint dust (Figure 1; Nored *et al* 2017). Briefly, paint dust polydisperse particles were generated from manually coated wood panels using an orbital sander in a polyvinylchloride glove box chamber (115 cm x 60 cm x 60cm) (Lancs Industries, Kirkland, WA). The efficiency of four membranes to collect TiO_2-containing paint dust was assessed by monitoring the size distribution of generated paint dust in the CARES (i.e., upstream) and after the membrane (i.e., downstream) for 5 min, simultaneously, and repeated at least six times (using a new wood panel each time) in order to get reproducible and accurate measurements. The collection efficiency of the four membranes was tested at face velocity of 1.92 cm/s. In addition, the collection efficiency of cellulose acetate membrane was measured at flow rates (Q: from 2 to 6 L/min) corresponding to face velocity of 1.92 to 5.76 cm/s and Reynolds number (Re) from 60 to 180.

The real-time 10-stage Quartz Crystal Microbalance (QCM) cascade impactor system (Model PC-2H, California, US) was used to measure particle mass in ten stages with 50% cut-off aerodynamic diameter cut-off points of 14, 9.7, 4.2, 2.8, 1.4, 0.7, 0.45, 0.30, 0.16 and 0.10 μm at 2 L/min flow rate. The average sensitivity is 1.4 ng per Hz but varies for each impactor stage because of differences in particle deposition in each stage. For typical ambient conditions, the signal-to-noise (S/N) ratio was more than 20, sufficient to adequately measure particle mass without crystal overloading. The impaction substrates (i.e., sensing crystals) were cleaned between experiments with n-hexane, and re-calibrated per manufacturer's protocol. In addition, the agreement between the two instruments was

also assessed at the beginning and end of each experiment using indoor air for 15-20 minutes.

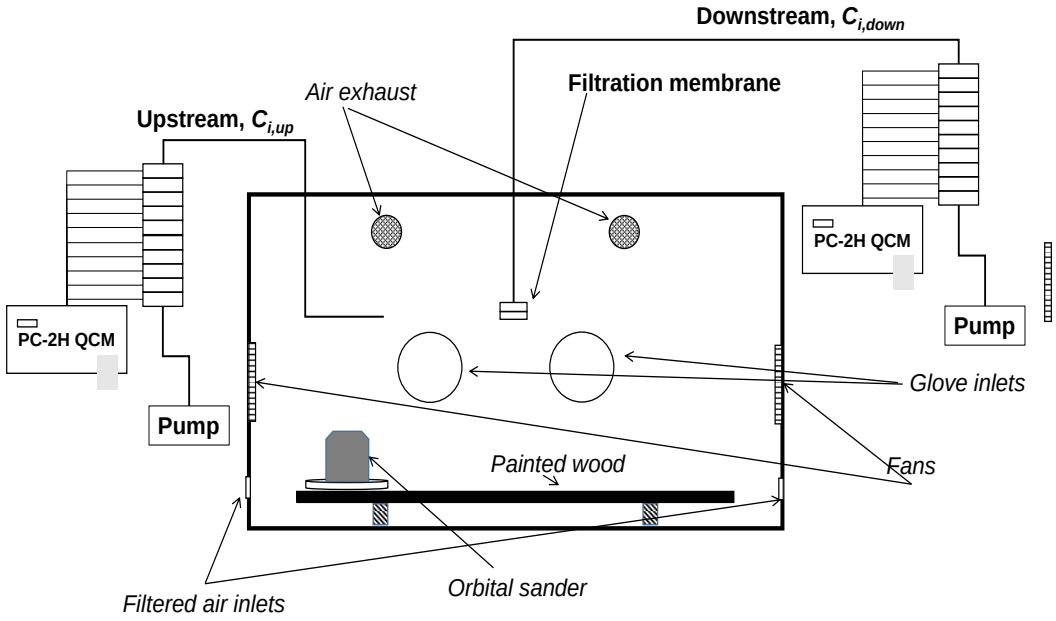

Figure 1. Schematic diagram of the experimental apparatus. Paint dust is generated into the chamber. The generated aerosol is measured in the chamber (Upstream, $C_{i,up}$) and after the filtration membrane (Downstream, $C_{i,down}$).

Total and size-dependent collection efficiency

The total (E_t) and size-dependent (E_i) collection efficiencies (dimensionless) were calculated using downstream ($C_{i,down}$) and upstream ($C_{i,up}$) particle mass concentrations as follows:

$$E_t = 1 - \frac{\sum_{i=1}^{10} C_{i,down}}{\sum_{i=1}^{10} C_{i,up}} \quad (1)$$

and

$$E_i = 1 - \frac{C_{i,down}}{C_{i,up}} \quad (2)$$

Statistical analysis

Particle mass concentrations were tested for normality using the Shapiro-Wilk test. The significance of difference in mean particle mass concentration values between groups was examined with the non-parametric Mann-Whitney (when two groups where compared) and Kruskal-Wallis (for more than two groups) tests at α=0.05. These tests were followed by Tukey's Honestly Significant Difference test. All analyses were done using SPSS (Version 25) (IBM Analytics, Armonk, NY) and Origin Pro (version 9.1) (OriginLab, Northampton, MA).

RESULTS

Figure 2 shows the representative relative size distribution of TiO_2-containing paint dust mass concentration in the CARES system (upstream) and after the cellulose acetate membrane (downstream). The total particle mass concentration was 540 ± 60 μg/m^3 for upstream and 17 ± 1 μg/m^3 for downstream ($p < 0.001$). The upstream concentration was comparable to that computed for paint dust using the same experimental configuration previously (864 ± 503 μg/m^3; Nored *et al* 2018). Particles in the accumulation mode range (100 nm – 1.4 μm) accounted for most of the upstream paint dust mass (ca. 61%) but less than 35% of downstream paint dust mass. Note that particles with diameter < 100 nm account for a small fraction of particles by mass but their particle number concentration is 2-3 orders of magnitude higher than particles with diameter < 1 μm (Nored *et al* 2018).

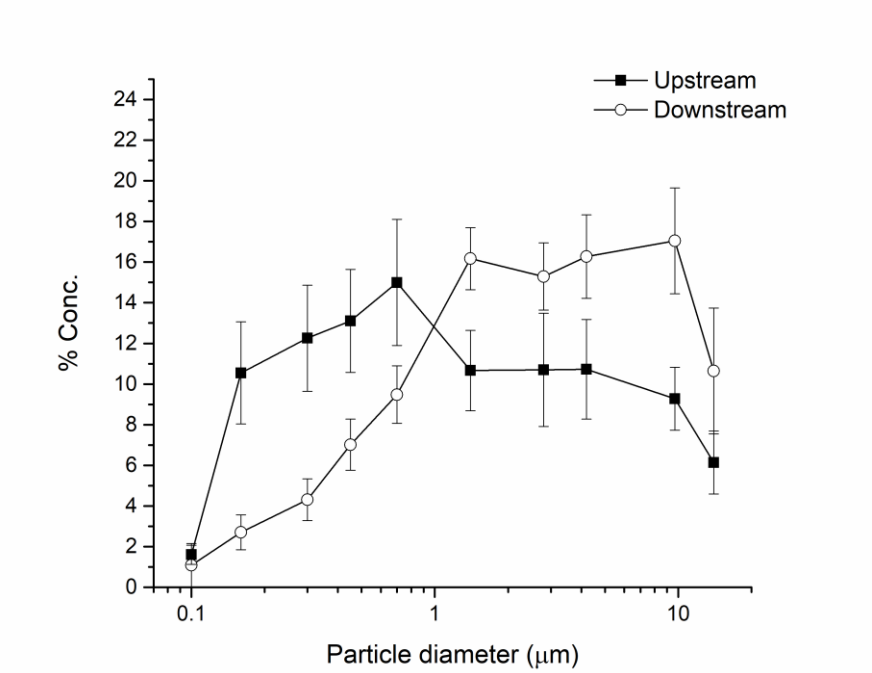

Figure 2. Percent relative mass (to the total particle mass) concentration of polydisperse paint dust aerosol upstream and downstream of cellulose acetate membrane at a face velocity of 1.92 cm/s in the CARES system. Squares and circles represent the average of at least six replicates of upstream and downstream concentration measured simultaneously. Error bars corresponds to 1.96 × standard error.

The collection efficiencies (E_t, dimensionless) as a function of particle size of each membrane at face velocity of 1.92 cm/s are shown in Figure 3. We compared polypropylene, the filter media used for the NIOSH-recommended N95 FFRs, PTFE and cellulose acetate membranes that are typically used for the collection of atmospheric aerosols.

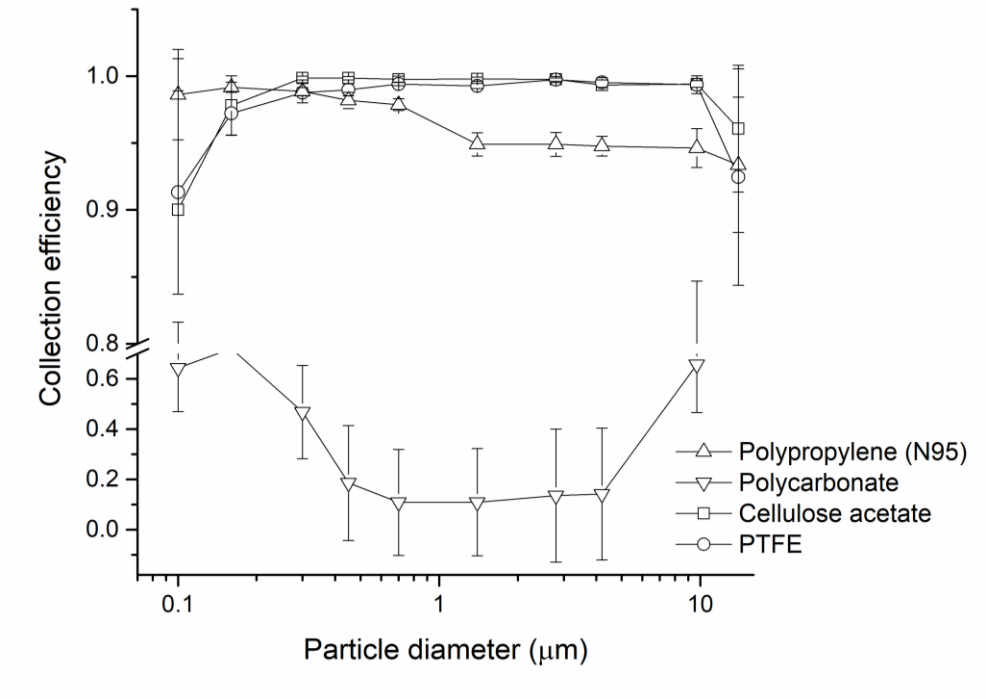

Figure 3. Collection efficiencies of polydisperse paint dust aerosol upstream and downstream of various membranes at a face velocity of 1.92 cm/s in the CARES system. Squares, circles, and triangles represent the average of at least six replicates of upstream and downstream concentration measured simultaneously. Error bars corresponds to 1.96 × standard error.

In addition, we also measured the collection efficiency of a porous polycarbonate membrane (pore size 8 μm). The polycarbonate membrane showed the poorest collection efficiency allowing for the penetration of most of the particles in the 0.45 – 9.7 μm size range (efficiencies varied from 11.6 % to 75%) due to its large pore size. Cellulose acetate and PFTE membranes filtered above 300 nm particles with efficiencies > 99% and rapidly declined for smaller particle sizes. In comparison, the filtration efficiency of N-95 polypropylene membrane increased as particle size decreased with the highest efficiencies (i.e., 96-99%) computed for particles below 150 nm. Particles above 10 μm were less efficiently collected (90-95%) by all membranes.

Table I. Filtration Efficiencies of Various Membranes at Flow Rates of 2, 4 and 6 L/min

Filter material	***Pore size***	***Q (L/min)***	***U (cm/sec)***	***% E_t***	***% $E_{<300}$***	***% $E_{<100}$***
Polypropylene (N95)	n/a	2.0	1.92	96.8 ± 18.8	98.9 ± 4.2	98.6 ± 1.2
Polycarbonate	8 μm	2.0	1.92	11.6 ± 38.3	64.1 ± 26.8	64.3 ± 8.2
Polytetrafluoroethylene	2 μm	2.0	1.92	99.5 ± 12.4	99.6 ± 8.4	91.3 ± 3.2
Cellulose acetate	0.2 μm	2.0	1.92	99.7 ± 16.0	99.6 ± 13.1	90.0 ± 4.7
Cellulose acetate	0.2 μm	4.0	3.84	99.1 ± 10.7	99.1 ± 5.3	93.6 ± 1.9
Cellulose acetate	0.2 μm	6.0	5.76	99.5 ± 1.6	99.2 ± 1.0	95.8 ± 3.6

Table I summarizes the key findings of the efficiencies for all particles (E_t), and particles with diameter < 300 ($E_{<300}$) and < 100 ($E_{<100}$) nm of the membranes at different face velocities. Polypropylene membrane performed as designed to collect more than 95% of the particles above 300 nm (96.8% ± 18.8%), but also particles below 300 nm (98.9% ± 4.2%). The collection efficiencies of both cellulose acetate and PTFE membranes were superior (more than 99%) than that on polypropylene membranes for particles above and below 300 nm. However, the collection efficiencies for particles below 100 nm of cellulose acetate and PTFE membranes dropped to approximately 90% as compared to about 99% of polypropylene membranes.

Higher face velocities (3.84 ad 5.76 cm/s) did not change the already high filtration efficiencies of particles above 300 nm but increased the filtration efficiency of particles below 100 nm up to 96.8% ± 18.8% at 3.84 cm/s and 96.8% ± 18.8% at 5.76 cm/s (Figure 4). Despite the increase, they were still inferior to the polypropylene membrane for the filtration of particles below 100 nm.

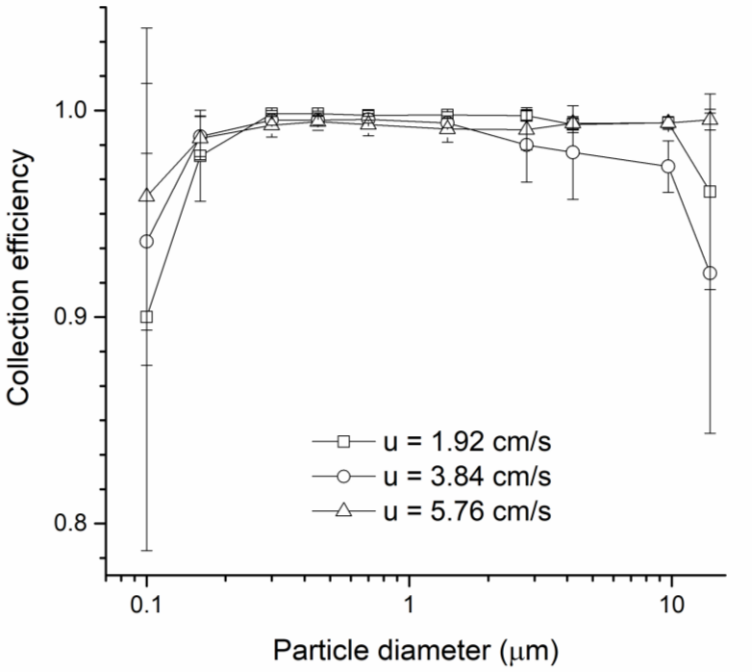

Figure 4. Collection efficiencies of polydisperse paint dust aerosol upstream and downstream of cellulose acetate at a face velocities of 1.92, 3.84 and 5.76 cm/s in the CARES system. Squares, circles, and triangles represent the average of at least six replicates of upstream and downstream concentration measured simultaneously. Error bars corresponds to 1.96 × standard error.

DISCUSSION

Commercially available personal protective equipment (PPEs), including N95 FFRs, are intended to efficiently remove airborne particles. The efficiency of the PPE depends on filtration variables such as face velocity, particle size, membrane material and porosity as well as the use-specific variables including proper fitting (i.e., the gap size between facial profiles and the PPE). Here, we examined the role of filtration variables on

the efficiencies of various membranes to remove polydisperse particles of paint-dust, specifically those containing TiO_2 at < 100 nm (Nored *et al* 2018).

It has been shown that total filtration efficiency for particles above 600 nm was high for small pore-size, non-absorbent, hydrophobic thermoplastic polymer-based membranes (Akalin *et al* 2010). Inertial impaction and gravitation sedimentation may be the dominant mechanism for particles above 1 μm. The filtration efficiency for particles above 1 μm increased as face velocities increases due to higher inertia. As particle size decreased from 1 μm to 100 nm, Brownian diffusion, and mechanical interception of particles by the filter fibers were the prevailing filtration mechanisms. Improved filtration efficiency may also be attributed to electrostatic attraction. The surface of TiO_2 NPs is found to be positive at pH less than 6.0 (Ramirez *et al* 2019) as compared to negatively charged PTFE and cellulose acetate (CH_3COO^-) membranes (He *et al* 2020). Polypropylene membranes are also considered electrostatic filters.

The filtration efficiency of particles below 300 nm was higher for PTFE and cellulose acetate than polypropylene membrane. The opposite was true for particles below 100 nm; the filtration efficiency of polypropylene membrane was higher than PTFE and cellulose acetate. It may be attributed to packing density, thickness, or fiber charge density in N95 FFRs polypropylene membranes as compared to thinner PTFE and cellulose acetate membranes (Huang *et al* 2013). It is noteworthy that diffusion and electrostatic attraction, the dominant mechanisms for the filtration of particles below 100 nm, differ for various conditions including face velocity and particle size, particularly in the nano-size range. For example, the electrostatic attraction is less effective as face velocity increases because of lower residence time (Givenhchi *et al* 2015). The thermal rebound effect, i.e., the

likelihood of particle detachment due to high thermal velocity and kinetic energy may further reduce the collection of particles below 100 nm at higher velocities. On the other hand, surface adhesion and elasticity, and the surface coating and potential to aggregate may limit thermal rebound and increase filtration efficiency for particles below 100 nm (Warheit *et al* 2008). In addition, the filtration of particles below 100 nm increase over time due to filter loading. It has been shown that the capture of particles below 100 nm increases with increasing the loading time through the formation of dendrite crystal on single fiber (Bahloul *et al* 2014).

CONCLUSIONS

We have measured the filtration efficiencies of various commonly used membranes to filter paint dust particles containing TiO2 NPs in the physiologically hazardous ~10nm to 300 nm size range. We found that cellulose acetate and PTFE membranes efficiently filtered more than 99% of particles above 300 nm by mass, albeit their efficiency declined for particles below 100 nm. On the other hand, packed polypropylene membranes obtained from N-95 masks showed filtration efficiencies slightly above 95% for particles above 300 nm, and higher filtration efficiency for particles below 300 and 100 nm. This may be attributed to the increased particle filtration by diffusion and electrostatic attraction in packed polypropylene membranes. The increase of the filtration efficiency of particles below 100 nm for PTFE and cellulose acetate membranes for higher face velocities may be due to the loading effect of previously collected particles in high concentration paint dust conditions.

REFERENCES

Akalin, M.; Usta, I.; Kocak, D.; Ozen, M.; (2010) Investigation of the filtration properties of medical masks *Medical and Healthcare Textiles* 93-97.

Baan, R,A., (200&) Carcinogenic hazards from inhaled carbon black, titanium dioxide, and talc not containing asbestos or asbestiform fibers: recent evaluations by an IARC Monographs Working Group. Inhalation Toxicology 2007;19 Suppl 1:213-228.

Bahloul, A.; Mahdavi, A.; Haghighat, F.; Ostiguy, C., (2014) Evaluation of N95 filtering facepiece respirator efficiency with cyclic and constant flows. *Journal of Occupational and Environmental Hygiene* 11(8):499-508.

Bałazy, A.; Toivola, M.; Reponen, T.; Podgórski, A.; Zimmer, A.; Grinshpun, S.A., (2005) Manikin-based performance evaluation of N95 filtering-facepiece respirators challenged with nanoparticles. Annals of Occupational Hygiene 50, 259–269.

Dankovic, D.; Kuempel, E.; Wheeler, M., (2007). An approach to risk assessment for TiO2. Inhalation Toxicology 19, 205-212.

Eninger, R.M.; Honda, T.; Adhikari, A.; Heinonen-Tanski, H.; Reponen, T.; Grinshpun, S.A., (2008) Filter Performance of N99 and N95 Facepiece Respirators Against Viruses and Ultrafine Particles. Annals of Occupational Hygiene.52, 385–396.

Eydner, M.; Schaudien, D.; Creutzenberg, O.; Ernst, H.; Hansen, T.; Baumgärtner, W.; Rittinghausen, S., (2012) Impacts after inhalation of nano- and fine-sized titanium dioxide particles: morphological changes, translocation within the rat lung, and evaluation of particle deposition using the relative deposition index. Inhalation Toxicology, 24:9, 557-569, DOI: 10.3109/08958378.2012.697494

Fryzek, J.P.; Chadda, B.; Marano, D.; White, K.; Schweitzer, S.; McLaughlin, J.K.; Blot, W.J., (2003) A cohort mortality study among titanium dioxide manufacturing workers in the United States. Journal of Occupational and Environmental Medicine 45(4):400-409.

Geiser, M.; Kreyling, W.G., (2010) Deposition and biokinetics of inhaled nanoparticles. Particle Fibre Toxicology 7, 2. https://doi.org/10.1186/1743-8977-7-2

Givehchi, R.; Li, Q.; Tan, T., (2015) The effect of electrostatic forces on filtration efficiency of granular filters, *Powder Technology* 277, 135-140.

He, W.; Zhao, Y-B.; Jiang, F.; Guo, Y.; Gao, H.; Liu, J.; Wang, J., (2020) Filtration performance and charge degradation during particle loading and reusability of charged PTFE needle felt filters. Separation and Purification Technology, 233, 116003.

Heinrich, U.; Fuhst, R.; Rittinghausen, S.; Creutzenberg, O.; Bellmann, B.; Koch, W.; Levsen, K., (1995) Chronic Inhalation Exposure of Wistar Rats and two Different Strains of Mice to Diesel Engine Exhaust, Carbon Black, and Titanium Dioxide,

Inhalation Toxicology, 7:4, 533-556.

Huang, S.-H; Chen, C.-W.; Kuo, Y.-M.; Lai, C.-Y.; McKay, R.; Chen, C.-C., (2013) Factors affecting filter penetration and quality factor of particulate respirators. Aerosol Air Quality and Research 13(1), 162-171.

Koponen, I.M.; Jensen, K.A.; Schneider, T., (2011) Comparison of dust released from sanding conventional and nanoparticle-doped wall and wood coatings. *Journal of Exposure Science and Environmental Epidemiology 21*:408–418.

Lee, J. H.; Kwon, M.; Ji, J. H.; Kang, C. S.; Ahn, K. H.; Han, J. H.; Yu, I. J., (2011). Exposure assessment of workplaces manufacturing nanosized TiO2 and silver. Inhalation toxicology, 23(4), 226–236.

Lim, S.S.; Vos, T.; Flaxman, A.D.; Danaei, G.; Shibuya, K.; Adair-Rohani, H., (2012) A comparative risk assessment of burden of disease and injury attributable to 67 risk factors and risk factor clusters in 21 regions, 1990–2010: a systematic analysis for the Global Burden of Disease Study Lancet. 380(9859):2224–2260.

Muller, C.; Sampson, R.J.; Winter, A.S., (2018) Environmental Inequality: The Social Causes and Consequences of Lead Exposure. *Annual Review of Sociology* 44:1, 263-282.

NIOSH. Current Intelligence Bulletin 63. Cincinnati: National Institute for Occupational Safety and Health; 2011. Occupational Exposure to Titanium Dioxide.

Nored, A.W.; Chalbot, M.C-C.G.; Kavouras, I.G., (2018) Characterization of paint dust aerosol generated from mechanical abrasion of TiO2-containing paints, *Journal of Occupational and Environmental Hygiene* 15:9, 629-640, DOI: 10.1080/15459624.2018.1484126.

Ortlieb, M., (2010). White Giant or White Dwarf?: Particle Size Distribution Measurements of TiO2. *GIT Laboratory Journal Europe*, 14, 42-43.

Ramirez, L.; Ramseier Gentile, S.; Zimmermann, S.; Stoll, S., (2019) Behavior of TiO_2 and CeO_2 Nanoparticles and Polystyrene Nanoplastics in Bottled Mineral, Drinking and Lake Geneva Waters. Impact of Water Hardness and Natural Organic Matter on Nanoparticle Surface Properties and Aggregation. *Water 11*, 721. https://doi.org/10.3390/w11040721

Ringen, K.; Dement, J.; Welch, L.; Dong, X.S.; Bingham, E.; Quinn, P.S.,(2014) Risks of a lifetime in construction. Part II: Chronic occupational diseases. American Journal of Industrial Medicine 57(11):1235–45.

Trochimowicz, H.J.; Lee, K.P.; Reinhardt, C.F., (1988). Chronic inhalation exposure of rats to titanium dioxide dust. Journal of Applied Toxicology, 8:383–385.

Wang, X.; Dong, X.S.; Welch, L.; Largay, J.; (2016) Respiratory Cancer and Non-Malignant Respiratory Disease-Related Mortality among Older Construction Workers-Findings from the Health and Retirement Study. Occupational and

Medical Health Affairs 4:235.

Warheit, D.B.; Sayes, C.M.; Reed, K.L.; Swain, K.A., (2008) Health effects related to nanoparticle exposures: environmental, health and safety considerations for assessing hazards and risks. Pharmacology Therapies 120(1), 35-42.

West, G.H.; Lippy, B.E.; Cooper, M.R.; Marsick, D.; Burrelli, L.G.; Griffin, K.N.; Segrave, A.M., (2016) Toward responsible development and effective risk management of nano-enabled products in the U.S. construction industry. Journal of Nanoparticle Research 18(2), 1-27.

GENERAL CONCLUSIONS

This work was a combination of two risk assessments and a modification to an already existing piece of equipment to raise the safety for construction workers. The first risk assessment determined the morphological characteristics of new nanoparticle infused paint. The SEM images of collected aerosol and settled dust indicated that individual nanoparticles do break free of the binder and are free floating particles in the aerosol There was also an indication of ENMs not breaking completely free of the binding agglomerates, but still being exposed and able to interact with the environment, albeit at a reduced rate. The chemical composition of the aerosol shows no loss of ENMs compared to fresh paint samples, with higher compositions of the dust being made up of ENMS with an increase in the coatings. Particle counters indicate with finer grit sandpaper there is an average of 9.5% of generated paint particles by mass are in the breathable size, and 20% of that mass was in the nano-size range. This indicates that there is a reasonable risk of exposure to the construction painter during the abrasion process.

The second risk assessment was the weathering of the same paint. The chemical and morphological analysis of the weathered pint samples indicated a loss of a significant portion of the ENMs in the paint. After three months of the weathering study the amount of ENMs in the aerosol or settled dust of a sample had a drop of more than 60%. At the end of the weathering study the loss of ENMs was even higher. The PNC has decreased, and all sizes of PM have also decreased substantially during the weatherization study. It is demonstrable that construction workers are not at a significant risk of exposure to

nanoparticles while sanding paint that has been weathered for more than a one-year increment.

The weatherization risk assessment did show that the leaching of the TiO_2 into may cause problems with the environment due to exposure. There was also a component of the second risk assessment focusing on the effects of pollution on paint containing nanoparticles. There was a significant amount of data that says that acid deposition and other pollutants does affect the paint and participates in the degrading process. CO, one of the variables that was tested for at the EPA site, has been shown in other studies to have no significant effect on paint in any way, so it must be acting the part of an intercept for all the chemicals that were not tested for in this study. It is important to note that a large percentage of the overall degradation of paint due to weathering was attributed to CO. This indicates that a more detailed environmental chemistry study would help understand the effects that happened to the paint during the weatherization study.

During the modification to the N95 research, the original polypropylene filter did very well. It exceeded the numbers previously found for it in independent studies. This research found the polypropylene filter never dropped below 95% collection efficiency throughout the study and had a collection efficiency at 98.6% below 100 nms. This collection efficiency dropped off above 300 nms. Where both PTFE and cellulose acetate became the better filter. Subsequent studies with change in face velocity showed an increase in collection efficiency at higher face velocities for cellulose acetate. The overall data shows that both PTFE and cellulose acetate had an overall higher collection efficiency compared to the original N95 filter.

This study has shown that the implementation of a PTFE or cellulose acetate layer, in conjunction with the N95 respirator, will help improve overall collection efficiency, especially in the target range of this study, which was below 300 nms.

Future Studies

There are several directions that future studies can be directed from this dissertation. TiO_2 needs be researched to greater depths. The mass balance of TiO_2 across product lifecycles in real environmental conditions should be researched. With the showing of this study of most of the nano sized TiO_2 escaping from paint in under a year, there should be a focus on where it all goes, to help prevent situations from forming in the future.

Other products besides paint should also be considered for this study, with an emphasis on pathways and length of time for escape. Other issues with specifically paint containing TiO_2 would be a more in-depth evaluation of pollution effects on the paint. Several chemicals could be hiding under the intercept that was CO in this study. Determining the individual chemicals of the pollution that helped break down paint, as well as the sources for those chemicals would be helpful for further risk assessment and evaluation of other materials.

One last direction for further studies is the fitting efficacy of FFRs. This work as well as several articles have shown that the respirator fit and the size of gaps in respirator protection massively effect the number of particles that can enter the breathing zone. Most of those articles focused on monodisperse methods with little emphasis on particles

in the nanoparticle size range. A polydisperse approach as well as a focus on the particles not traditionally tested for may provide new insights.

GENERAL REFERENCES

[1] Buzea C, Pacheco II, Robbie K. Nanomaterials and nanoparticles: Sources and toxicity. Biointerphases 2007;2:MR17–71.

[2] Hanus MJ, Harris AT. Nanotechnology innovations for the construction industry. Progress in Materials Science 2013;58:1056–102. https://doi.org/10.1016/j.pmatsci.2013.04.001.

[3] West GH, Lippy BE, Cooper MR, Marsick D, Burrelli LG, Griffin KN, et al. Toward responsible development and effective risk management of nano-enabled products in the U.S. construction industry. Journal of Nanoparticle Research 2016;18:1–27. https://doi.org/10.1007/s11051-016-3352-y.

[4] Lee J, Mahendra S, Alvarez PJJ. Nanomaterials in the construction industry: A review of their applications and environmental health and safety considerations. ACS Nano 2010;4. https://doi.org/10.1021/nn100866w.

[5] Buzea C, Pacheco II, Robbie K. Nanomaterials and nanoparticles: Sources and toxicity. Biointerphases 2007;2:MR17–71.

[6] Koponen IK, Jensen KA, Schneider T. Comparison of dust released from sanding conventional and nanoparticle-doped wall and wood coatings. Journal of Exposure Science and Environmental Epidemiology 2011;21:408–18. https://doi.org/10.1038/jes.2010.32.

[7] Hincapié I, Caballero-Guzman A, Hiltbrunner D, Nowack B. Use of engineered nanomaterials in the construction industry with specific emphasis on paints and their flows in construction and demolition waste in Switzerland. Waste Management 2015;43:398–406. https://doi.org/10.1016/J.WASMAN.2015.07.004.

[8] Gomez V, Levin M, Saber AT, Irusta S, Maso MD, Hanoi R, et al. Comparison of dust release from epoxy and paint nanocomposites and conventional products during sanding and sawing. Annals of Occupational Hygiene 2014;58:983–94. https://doi.org/10.1093/annhyg/meu046.

[9] Pilotek S, Tabellion F. Nanoparticles in coatings. European Coatings Journal 2005:170–6.

[10] Saison C, Perreault F, Daigle J-C, Fortin C, Claverie J, Morin M, et al. Effect of core–shell copper oxide nanoparticles on cell culture morphology and

photosynthesis (photosystem II energy distribution) in the green alga, Chlamydomonas reinhardtii. Aquatic Toxicology 2010;96:109–14.

[11] Kaegi R, Sinnet B, Zuleeg S, Hagendorfer H, Mueller E, Vonbank R, et al. Release of silver nanoparticles from outdoor facades. Environmental Pollution 2010;158:2900–5. https://doi.org/10.1016/j.envpol.2010.06.009.

[12] Piccinno F, Gottschalk F, Seeger S, Nowack B. Industrial production quantities and uses of ten engineered nanomaterials in Europe and the world. Journal of Nanoparticle Research 2012;14:1109. https://doi.org/10.1007/s11051-012-1109-9.

[13] Künniger T, Gerecke AC, Ulrich A, Huch A, Vonbank R, Heeb M, et al. Release and environmental impact of silver nanoparticles and conventional organic biocides from coated wooden façades. Environmental Pollution 2014;184:464–71. https://doi.org/10.1016/j.envpol.2013.09.030.

[14] Mohajerani A, Burnett L, Smith J V, Kurmus H, Milas J, Arulrajah A, et al. Nanoparticles in Construction Materials and Other Applications, and Implications of Nanoparticle Use. Materials (Basel, Switzerland) 2019;12:3052. https://doi.org/10.3390/ma12193052.

[15] Karlsson HL, Cronholm P, Gustafsson J, Möller L. Copper oxide nanoparticles are highly toxic: A comparison between metal oxide nanoparticles and carbon nanotubes. Chemical Research in Toxicology 2008;21:1726–32. https://doi.org/10.1021/tx800064j.

[16] Al-Kattan A, Wichser A, Vonbank R, Brunner S, Ulrich A, Zuin S, et al. Release of TiO2 from paints containing pigment-TiO2 or nano-TiO2 by weathering. Environmental Science: Processes & Impacts 2013;15:2186. https://doi.org/10.1039/c3em00331k.

[17] Giraldo AL, Peñuela GA, Torres-Palma RA, Pino NJ, Palominos RA, Mansilla HD. Degradation of the antibiotic oxolinic acid by photocatalysis with TiO2 in suspension. Water Research 2010;44:5158–67. https://doi.org/https://doi.org/10.1016/j.watres.2010.05.011.

[18] Bahnemann DW, Kholuiskaya SN, Dillert R, Kulak AI, Kokorin AI. Photodestruction of dichloroacetic acid catalyzed by nano-sized TiO2 particles. Applied Catalysis B: Environmental 2002;36:161–9. https://doi.org/https://doi.org/10.1016/S0926-3373(01)00301-0.

[19] Zheng S, Cai Y, O'Shea KE. TiO2 photocatalytic degradation of phenylarsonic acid. Journal of Photochemistry and Photobiology A: Chemistry 2010;210:61–8.

[20] Marolt T, Škapin AS, Bernard J, Živec P, Gaberšček M. Photocatalytic activity of anatase-containing facade coatings. Surface and Coatings Technology 2011;206:1355–61. https://doi.org/https://doi.org/10.1016/j.surfcoat.2011.08.053.

[21] Chen J, Poon C-S. Photocatalytic activity of titanium dioxide modified concrete materials – Influence of utilizing recycled glass cullets as aggregates. Journal of Environmental Management 2009;90:3436–42. https://doi.org/https://doi.org/10.1016/j.jenvman.2009.05.029.

[22] Gottschalk F, Sonderer T, Scholz RW, Nowack B. Modeled environmental concentrations of engineered nanomaterials (TiO2, ZnO, Ag, CNT, fullerenes) for different regions. Environmental Science & Technology 2009;43:9216–22.

[23] An J, Zhang M, Wang S, Tang J. Physical, chemical and microbiological changes in stored green asparagus spears as affected by coating of silver nanoparticles-PVP. LWT-Food Science and Technology 2008;41:1100–7.

[24] Batley GE, Kirby JK, McLaughlin MJ. Fate and risks of nanomaterials in aquatic and terrestrial environments. Accounts of Chemical Research 2012;46:854–62.

[25] Mohajerani A, Burnett L, Smith J V, Kurmus H, Milas J, Arulrajah A, et al. Nanoparticles in Construction Materials and Other Applications, and Implications of Nanoparticle Use. Materials (Basel, Switzerland) 2019;12:3052. https://doi.org/10.3390/ma12193052.

[26] Kaiser JP, Diener L, Wick P. Nanoparticles in paints: A new strategy to protect façades and surfaces? Journal of Physics: Conference Series, vol. 429, IOP Publishing; 2013, p. 012036.

[27] Brochocka A, Makowski K, Majchrzycka K, Grzybowski P. Efficiency of filtering materials used in respiratory protective devices against nanoparticles. International Journal of Occupational Safety and Ergonomics 2013;19:285–95.

[28] De Jong WH, Borm PJ a. Drug delivery and nanoparticles:applications and hazards. International Journal of Nanomedicine 2008;3:133–49. https://doi.org/10.2147/IJN.S596.

[29] Oberdörster G, Oberdörster E, Oberdörster J. Nanotoxicology: An emerging discipline evolving from studies of ultrafine particles. Environmental Health Perspectives 2005;113:823–39. https://doi.org/10.1289/ehp.7339.

[30] Hoet PH, Brüske-Hohlfeld I, Salata O V. Nanoparticles – known and unknown health risks. Journal of Nanobiotechnology 2004;2:12. https://doi.org/10.1186/1477-3155-2-12.

[31] Byrne JD, Baugh JA. The significance of nanoparticles in particle-induced pulmonary fibrosis. McGill Journal of Medicine : MJM : An International Forum for the Advancement of Medical Sciences by Students 2008;11:43–50.

[32] U.S. Department of Labor. Bureau of Labor Statistics (BLS), Occupational Outlook Handbook, 2016-17 Edition, Painters, Construction and Maintenance,. Occupational Outlook Handbook 2017:1. https://www.bls.gov/ooh/construction-

and-extraction/painters-construction-and-maintenance.htm (accessed January 1, 2017).

[33] Lim SS, Vos T, Flaxman AD, Danaei G, Shibuya K, Adair-Rohani H, et al. A comparative risk assessment of burden of disease and injury attributable to 67 risk factors and risk factor clusters in 21 regions, 1990–2010: a systematic analysis for the Global Burden of Disease Study 2010. The Lancet 2012;380:2224–60.

[34] IARC Working Group on the Evaluation of Carcinogenic Risks to Humans. Painting, firefighting, and shiftwork. IARC Monographs on the Evaluation of Carcinogenic Risks to Humans / World Health Organization, International Agency for Research on Cancer 2010;98:9–764.

[35] Guha N, Merletti F, Steenland NK, Altieri A, Cogliano V, Straif K. Lung cancer risk in painters: A meta-analysis. Environmental Health Perspectives 2010;118:303–12. https://doi.org/10.1289/ehp.0901402.

[36] Wang X, Dong XS, Welch L, Largay J. Respiratory Cancer and Non-Malignant Respiratory Disease-Related Mortality among Older Construction Workers-Findings from the Health and Retirement Study. Occupational Medicine & Health Affairs 2016;4:235. https://doi.org/10.4172/2329-6879.1000235.

[37] Ringen K, Dement J, Welch L, Dong XS, Bingham E, Quinn PS. Risks of a lifetime in construction. Part II: Chronic occupational diseases. American Journal of Industrial Medicine 2014;57:1235–45.

[38] Kaukiainen A, Martikainen R, Riala R, Reijula K, Tammilehto L. Work tasks, chemical exposure and respiratory health in construction painting. American Journal of Industrial Medicine 2008;51:1–8. https://doi.org/10.1002/ajim.20537.

[39] OSHA. TABLE Z-1 Limits for Air Contaminants n.d. https://www.osha.gov/laws-regs/regulations/standardnumber/1910/1910.1000TABLEZ1 (accessed October 10, 2018).

[40] Hinds WC. Aerosol technology: properties, behavior, and measurement of airborne particles. John Wiley & Sons; 1982.

[41] Eninger RM, Honda T, Adhikari A, Heinonen-Tanski H, Reponen T, Grinshpun SA. Filter Performance of N99 and N95 Facepiece Respirators Against Viruses and Ultrafine Particles. The Annals of Occupational Hygiene 2008;52:385–96.

[42] Rengasamy S, Eimer BC. Total Inward Leakage of Nanoparticles Through Filtering Facepiece Respirators. The Annals of Occupational Hygiene 2011;55:253–63. https://doi.org/10.1093/annhyg/meq096.

[43] Bałazy A, Toivola M, Reponen T, Podgórski A, Zimmer A, Grinshpun SA. Manikin-based performance evaluation of N95 filtering-facepiece respirators challenged with nanoparticles. Annals of Occupational Hygiene 2005;50:259–69.

[44] LATHRACHE R; FH. Enhancement of particle deposition in filters due to electrostatic effects. Filtration & Separation 1987;24:418–22.